GEOMETRIZED VACUUM PHYSICS.
PART 10: NAKED "PLANETS" AND "STARS"

Mikhail Batanov-Gaukhman[1],

(1) Moscow Aviation Institute (National Research University),
Institute № 2 "Aircraft and rocket engines and power plants",
st. Volokolamsk highway, 4, Moscow – Russia, 125993
(e-mail: alsignat@yandex.ru)

ABSTRACT

This article is the tenth part of the scientific project under the general title "Geometrized Vacuum Physics Based on the Algebra of Signature " [1,2,3,4,5,6,7,8,9]. In this article, based on exact solutions of the extended Einstein vacuum equation, metric-dynamic models of stable spherical vacuum formations of planetary scale with a core radius of the order of $r_4 \sim 10^{7-} – 10^8$ cm = 100 – 1000 km are proposed. These electrically neutral vacuum formations are called naked "planets" and "stars". The concept of a naked "planet" implies that this article does not take into account the presence and influence of small vacuum formations (micro-, nano- and picoscopic "particles"), only curvatures of the vacuum of stellar-planetary scale are considered. In particular, metric-dynamic models of a naked "star" and naked "planets" of the Solar System are proposed. The analogy between the naked "Solar System" and a biological cell is shown. Like the entire project, this article is aimed at implementing the program of complete geometrization physics of Clifford-Einstein-Wheeler.

Keywords: vacuum physics, metric-dynamic models, geometrodynamics, vacuum, Algebra of signature, naked planets, naked stars, geometrization of physics.

BACKGROUND & INTRODUCTION

This is the tenth part of a series of articles under the general title "Geometrized Vacuum Physics (GVPh) based on the Algebra of Signatures (AS)". The previous eight articles are listed in the bibliography [1,2,3,4,5,6,7,8,9].

In the article [6] the "Hierarchical Cosmological Model" was proposed, which is developed on the basis of solutions of the third extended Einstein vacuum equation (11) in [6]

$$R_{ik} + ½\, g_{ik}\left(\sum_{m=1}^{\infty} \Lambda_m + \sum_{n=1}^{\infty} - \Lambda_n\right) = 0. \quad (1)$$

From this equation, one simplified and shortened "chain" of Λ_m-terms (where $\Lambda_m = 3/r_m^2$, here r_m is the radius of the m-th spherical vacuum formation) was extracted, consisting of only 10 links

$$\begin{cases} R_{ik} + g_{ik} \sum_{m=1}^{10} \Lambda_m = 0, \\ R_{ik} - g_{ik} \sum_{m=1}^{10} \Lambda_m = 0. \end{cases} \quad (2)$$

The metrics-solution of this system of equations have the form (23) – (34) in [6]:
- five metrics with the signature (+ – – –)

$$ds_1^{(+)2} = \left(1 - \frac{r_0}{r} + \frac{\Lambda_0 r^2}{3}\right) c^2dt^2 - \frac{dr^2}{\left(1 - \frac{r_0}{r} + \frac{\Lambda_0 r^2}{3}\right)} - r^2(d\theta^2 + sin^2\,\theta\, d\phi^2), \quad (3)$$

$$ds_2^{(+)2} = \left(1 + \frac{r_0}{r} - \frac{\Lambda_0 r^2}{3}\right) c^2dt^2 - \frac{dr^2}{\left(1 + \frac{r_0}{r} - \frac{\Lambda_0 r^2}{3}\right)} - r^2(d\theta^2 + sin^2\,\theta\, d\phi^2), \quad (4)$$

$$ds_3^{(+)2} = \left(1 - \frac{r_0}{r} - \frac{\Lambda_0 r^2}{3}\right) c^2dt^2 - \frac{dr^2}{\left(1 - \frac{r_0}{r} - \frac{\Lambda_0 r^2}{3}\right)} - r^2(d\theta^2 + sin^2\,\theta\, d\phi^2), \quad (5)$$

$$ds_4^{(+)2} = \left(1 + \frac{r_0}{r} + \frac{\Lambda_0 r^2}{3}\right) c^2dt^2 - \frac{dr^2}{\left(1 + \frac{r_0}{r} + \frac{\Lambda_0 r^2}{3}\right)} - r^2(d\theta^2 + sin^2\,\theta\, d\phi^2), \quad (6)$$

$$ds_5^{(+)2} = c^2dt^2 - dr^2 - r^2(d\theta^2 + sin^2\,\theta\, d\phi^2); \quad (7)$$

- и пять метрик с сигнатурой (– + + +)

$$ds_1^{(-)2} = -\left(1 - \frac{r_0}{r} + \frac{\Lambda_0 r^2}{3}\right) c^2 dt^2 + \frac{dr^2}{\left(1 - \frac{r_0}{r} + \frac{\Lambda_0 r^2}{3}\right)} + r^2(d\theta^2 + sin^2\,\theta\, d\phi^2), \quad (8)$$

$$ds_2^{(-)2} = -\left(1 + \frac{r_0}{r} - \frac{\Lambda_0 r^2}{3}\right) c^2 dt^2 + \frac{dr^2}{\left(1 + \frac{r_0}{r} - \frac{\Lambda_0 r^2}{3}\right)} + r^2(d\theta^2 + sin^2\,\theta\, d\phi^2), \quad (9)$$

$$ds_3^{(-)2} = -\left(1 - \frac{r_0}{r} - \frac{\Lambda_0 r^2}{3}\right) c^2 dt^2 + \frac{dr^2}{\left(1 - \frac{r_0}{r} - \frac{\Lambda_0 r^2}{3}\right)} + r^2(d\theta^2 + sin^2\,\theta\, d\phi^2), \quad (10)$$

$$ds_4^{(-)2} = -\left(1 + \frac{r_0}{r} + \frac{\Lambda_0 r^2}{3}\right) c^2 dt^2 + \frac{dr^2}{\left(1 + \frac{r_0}{r} + \frac{\Lambda_0 r^2}{3}\right)} + r^2(d\theta^2 + sin^2\,\theta\, d\phi^2), \quad (11)$$

$$ds_5^{(-)2} = -c^2 dt^2 + dr^2 + r^2(d\theta^2 + sin^2\,\theta\, d\phi^2), \quad (12)$$

where

$$\Lambda_0 = \sum_{m=1}^{10} \Lambda_m = \sum_{m=1}^{10} \frac{3}{r_m^2}, \quad (13)$$

$$r_0 = \sum_{m=1}^{10} r_m. \quad (14)$$

In [6] it was shown that the zero components and, accordingly, the denominators of the unit components of the metric tensor from the solution metrics (3) – (14) can be represented in the form (35) – (42) in [6]

$$1 - \frac{r_0}{r} + \frac{\Lambda_0 r^2}{3} = 1 - \frac{r_1 + r_2 + \cdots + r_{10}}{r} + \left(\frac{1}{r_1^2} + \frac{1}{r_2^2} + \cdots + \frac{1}{r_{10}^2}\right) r^2 = \quad (15)$$
$$= 1 + \left(1 - \frac{r_{10}}{r} + \frac{r^2}{r_9^2}\right) - \left(1 + \frac{r_9}{r} - \frac{r^2}{r_8^2}\right) + \left(1 - \frac{r_8}{r} + \frac{r^2}{r_7^2}\right) - \left(1 + \frac{r_7}{r} - \frac{r^2}{r_6^2}\right) + \left(1 - \frac{r_6}{r} + \frac{r^2}{r_5^2}\right) - \left(1 + \frac{r_5}{r} - \frac{r^2}{r_4^2}\right) + \left(1 - \frac{r_4}{r} + \frac{r^2}{r_3^2}\right) -$$
$$- \left(1 + \frac{r_3}{r} - \frac{r^2}{r_2^2}\right) + \left(1 - \frac{r_2}{r} + \frac{r^2}{r_1^2}\right) - \left(1 + \frac{r_1}{r} - \frac{r^2}{r_{10}^2}\right),$$

$$1 + \frac{r_0}{r} - \frac{\Lambda_0 r^2}{3} = 1 + \frac{r_1 + r_2 + \cdots + r_{10}}{r} - \left(\frac{1}{r_1^2} + \frac{1}{r_2^2} + \cdots + \frac{1}{r_{10}^2}\right) r^2 = \quad (16)$$
$$= 1 + \left(1 + \frac{r_{10}}{r} - \frac{r^2}{r_9^2}\right) - \left(1 - \frac{r_9}{r} + \frac{r^2}{r_8^2}\right) + \left(1 + \frac{r_8}{r} - \frac{r^2}{r_7^2}\right) - \left(1 - \frac{r_7}{r} + \frac{r^2}{r_6^2}\right) + \left(1 + \frac{r_6}{r} - \frac{r^2}{r_5^2}\right) - \left(1 - \frac{r_5}{r} + \frac{r^2}{r_4^2}\right) + \left(1 + \frac{r_4}{r} - \frac{r^2}{r_3^2}\right) -$$
$$- \left(1 - \frac{r_3}{r} + \frac{r^2}{r_2^2}\right) + \left(1 + \frac{r_2}{r} - \frac{r^2}{r_1^2}\right) - \left(1 - \frac{r_1}{r} + \frac{r^2}{r_{10}^2}\right),$$

$$1 - \frac{r_0}{r} - \frac{\Lambda_0 r^2}{3} = 1 - \frac{r_1 + r_2 + \cdots + r_{10}}{r} - \left(\frac{1}{r_1^2} + \frac{1}{r_2^2} + \cdots + \frac{1}{r_{10}^2}\right) r^2 = \quad (17)$$
$$= 1 + \left(1 - \frac{r_{10}}{r} - \frac{r^2}{r_9^2}\right) - \left(1 + \frac{r_9}{r} + \frac{r^2}{r_8^2}\right) + \left(1 - \frac{r_8}{r} - \frac{r^2}{r_7^2}\right) - \left(1 + \frac{r_7}{r} + \frac{r^2}{r_6^2}\right) + \left(1 - \frac{r_6}{r} - \frac{r^2}{r_5^2}\right) - \left(1 + \frac{r_5}{r} + \frac{r^2}{r_4^2}\right) + \left(1 - \frac{r_4}{r} - \frac{r^2}{r_3^2}\right) -$$
$$- \left(1 + \frac{r_3}{r} + \frac{r^2}{r_2^2}\right) + \left(1 - \frac{r_2}{r} - \frac{r^2}{r_1^2}\right) - \left(1 + \frac{r_1}{r} + \frac{r^2}{r_{10}^2}\right),$$

$$1 + \frac{r_0}{r} + \frac{\Lambda_0 r^2}{3} = 1 + \frac{r_1 + r_2 + \cdots + r_{10}}{r} + \left(\frac{1}{r_1^2} + \frac{1}{r_2^2} + \cdots + \frac{1}{r_{10}^2}\right) r^2 = \quad (18)$$
$$= 1 + \left(1 + \frac{r_{10}}{r} + \frac{r^2}{r_9^2}\right) - \left(1 - \frac{r_9}{r} - \frac{r^2}{r_8^2}\right) + \left(1 + \frac{r_8}{r} + \frac{r^2}{r_7^2}\right) - \left(1 - \frac{r_7}{r} - \frac{r^2}{r_6^2}\right) + \left(1 + \frac{r_6}{r} + \frac{r^2}{r_5^2}\right) - \left(1 - \frac{r_5}{r} - \frac{r^2}{r_4^2}\right) + \left(1 + \frac{r_4}{r} + \frac{r^2}{r_3^2}\right) -$$
$$- \left(1 - \frac{r_3}{r} - \frac{r^2}{r_2^2}\right) + \left(1 + \frac{r_2}{r} + \frac{r^2}{r_1^2}\right) - \left(1 - \frac{r_1}{r} - \frac{r^2}{r_{10}^2}\right),$$

$$-\left[1+\frac{r_0}{r}-\frac{\Lambda_0 r^2}{3}\right]=-\left[1-\frac{r_1+r_2+\cdots+r_{10}}{r}+\left(\frac{1}{r_1^2}+\frac{1}{r_2^2}+\cdots+\frac{1}{r_{10}^2}\right)r^2\right]= \tag{19}$$
$$=-1-\left(1-\frac{r_{10}}{r}+\frac{r^2}{r_9^2}\right)+\left(1+\frac{r_9}{r}-\frac{r^2}{r_8^2}\right)-\left(1-\frac{r_8}{r}+\frac{r^2}{r_7^2}\right)+\left(1+\frac{r_7}{r}-\frac{r^2}{r_6^2}\right)-\left(1-\frac{r_6}{r}+\frac{r^2}{r_5^2}\right)+\left(1+\frac{r_5}{r}-\frac{r^2}{r_4^2}\right)-\left(1-\frac{r_4}{r}+\frac{r^2}{r_3^2}\right)+$$
$$+\left(1+\frac{r_3}{r}-\frac{r^2}{r_2^2}\right)-\left(1-\frac{r_2}{r}+\frac{r^2}{r_1^2}\right)+\left(1+\frac{r_1}{r}-\frac{r^2}{r_{10}^2}\right),$$

$$-\left[1+\frac{r_0}{r}-\frac{\Lambda_0 r^2}{3}\right]=-\left[1+\frac{r_1+r_2+\cdots+r_{10}}{r}-\left(\frac{1}{r_1^2}+\frac{1}{r_2^2}+\cdots+\frac{1}{r_{10}^2}\right)r^2\right]= \tag{20}$$
$$=-1-\left(1+\frac{r_{10}}{r}-\frac{r^2}{r_9^2}\right)+\left(1-\frac{r_9}{r}+\frac{r^2}{r_8^2}\right)-\left(1+\frac{r_8}{r}-\frac{r^2}{r_7^2}\right)+\left(1-\frac{r_7}{r}+\frac{r^2}{r_6^2}\right)-\left(1+\frac{r_6}{r}-\frac{r^2}{r_5^2}\right)+\left(1-\frac{r_5}{r}+\frac{r^2}{r_4^2}\right)-\left(1+\frac{r_4}{r}-\frac{r^2}{r_3^2}\right)+$$
$$+\left(1-\frac{r_3}{r}+\frac{r^2}{r_2^2}\right)-\left(1+\frac{r_2}{r}-\frac{r^2}{r_1^2}\right)+\left(1-\frac{r_1}{r}+\frac{r^2}{r_{10}^2}\right),$$

$$-\left[1-\frac{r_0}{r}-\frac{\Lambda_0 r^2}{3}\right]=-\left[1-\frac{r_1+r_2+\cdots+r_{10}}{r}-\left(\frac{1}{r_1^2}+\frac{1}{r_2^2}+\cdots+\frac{1}{r_{10}^2}\right)r^2\right]= \tag{21}$$
$$=-1+\left(1-\frac{r_{10}}{r}-\frac{r^2}{r_9^2}\right)-\left(1+\frac{r_9}{r}+\frac{r^2}{r_8^2}\right)+\left(1-\frac{r_8}{r}-\frac{r^2}{r_7^2}\right)-\left(1+\frac{r_7}{r}+\frac{r^2}{r_6^2}\right)+\left(1-\frac{r_6}{r}-\frac{r^2}{r_5^2}\right)-\left(1+\frac{r_5}{r}+\frac{r^2}{r_4^2}\right)+\left(1-\frac{r_4}{r}-\frac{r^2}{r_3^2}\right)-$$
$$-\left(1+\frac{r_3}{r}+\frac{r^2}{r_2^2}\right)+\left(1-\frac{r_2}{r}-\frac{r^2}{r_1^2}\right)-\left(1+\frac{r_1}{r}+\frac{r^2}{r_{10}^2}\right),$$

$$-\left[1+\frac{r_0}{r}+\frac{\Lambda_0 r^2}{3}\right]=-\left[1+\frac{r_1+r_2+\cdots+r_{10}}{r}+\left(\frac{1}{r_1^2}+\frac{1}{r_2^2}+\cdots+\frac{1}{r_{10}^2}\right)r^2\right]= \tag{22}$$
$$=-1-\left(1+\frac{r_{10}}{r}+\frac{r^2}{r_9^2}\right)+\left(1-\frac{r_9}{r}-\frac{r^2}{r_8^2}\right)-\left(1+\frac{r_8}{r}+\frac{r^2}{r_7^2}\right)+\left(1-\frac{r_7}{r}-\frac{r^2}{r_6^2}\right)-\left(1+\frac{r_6}{r}+\frac{r^2}{r_5^2}\right)+\left(1-\frac{r_5}{r}-\frac{r^2}{r_4^2}\right)-\left(1+\frac{r_4}{r}+\frac{r^2}{r_3^2}\right)+$$
$$+\left(1-\frac{r_3}{r}-\frac{r^2}{r_2^2}\right)-\left(1+\frac{r_2}{r}+\frac{r^2}{r_1^2}\right)+\left(1-\frac{r_1}{r}-\frac{r^2}{r_{10}^2}\right).$$

Each term enclosed in brackets on the right-hand sides of Exs. (15) – (22), when substituted into metrics (3) – (12), is a separate Kottler solution of the second Einstein vacuum equation of the form

$$R_{ik}+g_{ik}\Lambda_m=0. \tag{23}$$

Within the framework of Geometricized Vacuum Physics (GVPh) – this means that the metric-solutions (3) – (12) describe stable spherical vacuum formations (see [5]).

Further, in the article [6], it was proposed that the radii r_m in Exs. (3) – (22) are members of a discrete hierarchical sequence of characteristic sizes of spherical formations (44a) in [6]:

$r_1 \sim 10^{39}$ cm is radius commensurate with the radius of the mega-Universe core; (44a)
$r_2 \sim 10^{29}$ cm is radius commensurate with the radius of the observable Universe core;
$r_3 \sim 10^{19}$ cm is radius commensurate with the radius of the galactic core;
$r_4 \sim 10^{7}$ cm is radius commensurate with the radius of the core of a planet or star;
$r_5 \sim 10^{-3}$ cm is radius commensurate with the radius of a biological cell;
$r_6 \sim 10^{-13}$ cm is radius commensurate with the radius of an elementary particle core;
$r_7 \sim 10^{-24}$ cm is radius commensurate with the radius of a proto-quark core;
$r_8 \sim 10^{-34}$ cm is radius commensurate with the radius of a plankton core;
$r_9 \sim 10^{-45}$ cm is radius commensurate with the radius of the proto-plankton core;
$r_{10} \sim 10^{-55}$ cm is radius commensurate with the size of the instanton core.

As a result, it turned out that metrics (3) – (12), taking into account Exs. (13) – (22), describe a metric-dynamic hierarchical cosmological model of a sequence of 10 spherical vacuum formations, nested inside each other like nesting dolls. That is, the internal nucleolus of each cores, in turn, is the core for the next nucleus, and so on up to ten iterations, as shown in Figure 1.

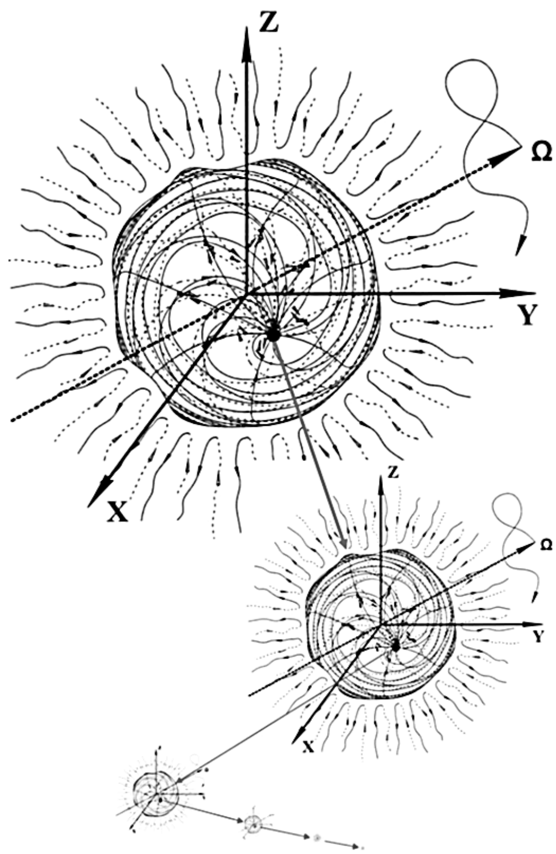

Fig. 1. (repetition of Figure 1 in [6]). Hierarchical sequence of spherical formations of different scales, nested inside each other like nesting dolls

In the articles [6,7,8,9], from the hierarchical sequence of spherical vacuum formations described by the set of metrics (3) – (12) taking into account Exs. (13) – (24), only one level of stable vacuum formations was singled out for consideration – the level of picoscopic "particles" (i.e. "particles" with a characteristic size of the nucleus of the order of $r_6 \sim 10^{-13}$ cm). In this case, a striking coincidence of the geometrized models of picoscopic “particles” with the currently accepted Standard Model of elementary particles was discovered.

In the works [6,7,8,9] it was repeatedly noted that everything written in these articles in relation to the level of picoscopic "particles" also applies to all other levels of the hierarchical cosmological model (see Figure 1), i.e. to "proto-quarks", "planets", "galaxies", etc. That is, the levels of organization of stable spherical vacuum formations of different scales are similar to each other.

However, the statement about the similarity of, for example, metric-dynamic models of picoscopic elementary "particles" and macroscopic "planets" met with complete misunderstanding of colleagues, whose thinking is conditioned by the modern scientific picture of the world. Therefore, in this article an attempt was made to isolate from the general hierarchical model (3) – (24) the level of macroscopic stable spherical vacuum formations of a planetary scale and to construct metric-dynamic models of naked "planets" and "stars".

MATERIALS AND METHOD

1 The concept of a naked "planet"

Within the framework of modern natural science, a planet (or star) is perceived as a dense accumulation of a huge number of elementary particles that are united into atoms, molecules, cells, organisms, liquids, stones, etc. (see Figure 2*a*).

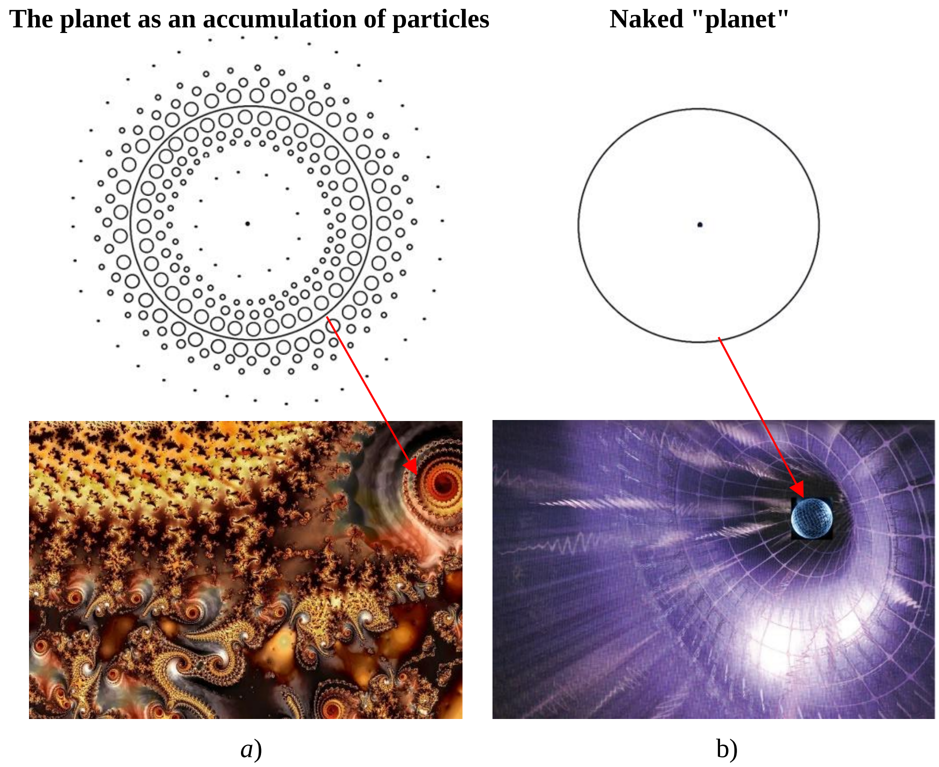

Fig. 2. *a*) Schematic and fractal illustrations of the planet as a huge accumulation of macro-, mini-, miro-, nano- and picoscopic local stable vacuum formations ("particles", "atoms", "molecules", "cells", etc.) in the vicinity of its core; *b*) Schematic representation and illustration of a stable spherical curvature of the $\lambda_{6,7}$-vacuum of a planetary scale, consisting of a core and an outer shell. This large-scale stable spherical $\lambda_{6,7}$-vacuum formation (conditionally cleared of small "particles") will be called a naked "planet"

In GTR, it is believed that this entire innumerable set of small particles has the ability to curve 4-dimensional space-time so that an absorbing space-time funnel is formed, which is usually considered to be the cause of gravity.

In the Geometrized Vacuum Physics (GVPh) developed here, on the contrary, the cause of gravity is a stable funnel-shaped curvature of the $\lambda_{6,7}$-vacuum (Figure 2*b*) (the definition of the $\lambda_{m,n}$-vacuum is given in §1 in [1]). This large-scale $\lambda_{6,7}$-vacuum funnel draws in "particles" (i.e. the smallest corpuscular $\lambda_{-12,-15}$-vacuum formations considered in [6]), clearing the surrounding space of them.

Before investigating the cause of gravity, which attracts a huge number of small "particles" to the core of the planet, it is first necessary to understand how the large-scale $\lambda_{6,7}$-vacuum is curved in the region of space under study.

For this, we introduce the concept of a naked "planet". By a naked "planet" we mean a large-scale stable spherical $\lambda_{6,7}$-vacuum formation with a characteristic core radius $r_4 \sim 100 - 1000$ km = $10^7 - 10^8$ cm (from hierarchy (24)), in the vicinity of which macro-, mini-, micro-, nano- and picoscopic local stable $\lambda_{m,n}$-vacuum formations are conditionally absent (see Figures 2*b* &3).

Fig. 3. Fractal illustrations of the outer shell of a naked "planet", i.e. a curved region of $\lambda_{6,7}$-vacuum, surrounding the core of a stable planetary $\lambda_{6,7}$-vacuum formation, from which all pico- and microscopic "particles" are conditionally removed

The definition of $\lambda_{6,7}$-vacuum as a 3-dimensional curved landscape, illuminated from the surrounding reality by light rays with a wavelength of $\lambda_{6,7}$ from the range of $\Delta\lambda = 10^6 – 10^7$ cm = 10 – 100 km (see §1 in [1]), initially suggests that the result of such probing in the case under consideration will be a naked "planet", since for 10 – 100-kilometer electromagnetic waves, small particles are not an obstacle. Such light rays reveal only the large-scale curvature of the surrounding space (vacuum). That is, geodetic lines of light rays with a wavelength of $\lambda_{6,7}$ from the range of 10 – 100 km immediately indicate a stable spherical formation (see Figure 2*b* and 3), which we call a naked "planet".

2 Naked planetary valence P_k-"quarks$_{10}$"

By analogy, as from metrics of the form (3) – (22) in §4.1 in [6] the metric-dynamic models of the "electron" and "positron" were isolated, we will leave in metrics (3) – (7) taking into account (15) – (18) for consideration only those terms that contain the radius $r_4 \sim 10^7$ cm = 100 km, commensurate with the radius of the core of the naked "planet". As a result, we obtain the following multilayer metric-dynamic model of a stable "convex" spherical $\lambda_{6,7}$-vacuum formation, which we will call a valence planetary Pe_y^+-"quark$_{10}$" (the index 10 means that this planetary Pe_y^+-"quark$_{10}$" is in a hierarchical chain of ten stable spherical $\lambda_{m,n}$-vacuum formations nested inside each other, see Figure 1):

The valence planetary Pe_y^+-"QUARK$_{10}$" (25)

Stable "convex" multilayer spherical curvature of $\lambda_{6,7}$-vacuum
with signature (+ – – –), consisting of:

The outer shell of the Pe_y^+-"quark$_{10}$"
in the interval [r_3, r_4] (see Figure 2*b* and 4)

I $$ds_1^{(+---)2} = \left(1 - \frac{r_4}{r} + \frac{r^2}{r_3^2}\right)c^2dt^2 - \frac{dr^2}{\left(1 - \frac{r_4}{r} + \frac{r^2}{r_3^2}\right)} - r^2(d\theta^2 + sin^2\,\theta\, d\phi^2), \quad (26)$$

H $$ds_2^{(+---)2} = \left(1 + \frac{r_4}{r} - \frac{r^2}{r_3^2}\right)c^2dt^2 - \frac{dr^2}{\left(1 + \frac{r_4}{r} - \frac{r^2}{r_3^2}\right)} - r^2(d\theta^2 + sin^2\,\theta\, d\phi^2), \quad (27)$$

V $$ds_3^{(+---)2} = \left(1 - \frac{r_4}{r} - \frac{r^2}{r_3^2}\right)c^2dt^2 - \frac{dr^2}{\left(1 - \frac{r_4}{r} - \frac{r^2}{r_3^2}\right)} - r^2(d\theta^2 + sin^2\,\theta\, d\phi^2), \quad (28)$$

H′ $$ds_4^{(+---)2} = \left(1 + \frac{r_4}{r} + \frac{r^2}{r_3^2}\right)c^2dt^2 - \frac{dr^2}{\left(1 + \frac{r_4}{r} + \frac{r^2}{r_3^2}\right)} - r^2(d\theta^2 + sin^2\,\theta\, d\phi^2); \quad (29)$$

The core of the *Pe*$_y^+$-"quark$_{10}$"
in the interval [r_4, r_5] (see Figure 2*b* and 4)

I $$ds_1^{(+---)2} = -\left(1 - \frac{r_5}{r} + \frac{r^2}{r_4^2}\right)c^2dt^2 - \frac{dr^2}{-\left(1 - \frac{r_5}{r} + \frac{r^2}{r_4^2}\right)} - r^2(d\theta^2 + \sin^2\theta\, d\phi^2), \quad (30)$$

H $$ds_2^{(+---)2} = -\left(1 + \frac{r_5}{r} - \frac{r^2}{r_4^2}\right)c^2dt^2 - \frac{dr^2}{-\left(1 + \frac{r_5}{r} - \frac{r^2}{r_4^2}\right)} - r^2(d\theta^2 + \sin^2\theta\, d\phi^2), \quad (31)$$

V $$ds_3^{(+---)2} = -\left(1 - \frac{r_5}{r} - \frac{r^2}{r_4^2}\right)c^2dt^2 - \frac{dr^2}{-\left(1 - \frac{r_5}{r} - \frac{r^2}{r_4^2}\right)} - r^2(d\theta^2 + \sin^2\theta\, d\phi^2), \quad (32)$$

H′ $$ds_4^{(+---)2} = -\left(1 + \frac{r_5}{r} + \frac{r^2}{r_4^2}\right)c^2dt^2 - \frac{dr^2}{-\left(1 + \frac{r_5}{r} + \frac{r^2}{r_4^2}\right)} - r^2(d\theta^2 + \sin^2\theta\, d\phi^2); \quad (33)$$

The substrate of the *Pe*$_y^+$-"quark$_{10}$"
in the interval [0, ∞]

i $$ds_5^{(+---)2} = c^2dt^2 - dr^2 - r^2(d\theta^2 + \sin^2\theta\, d\phi^2). \quad (34)$$

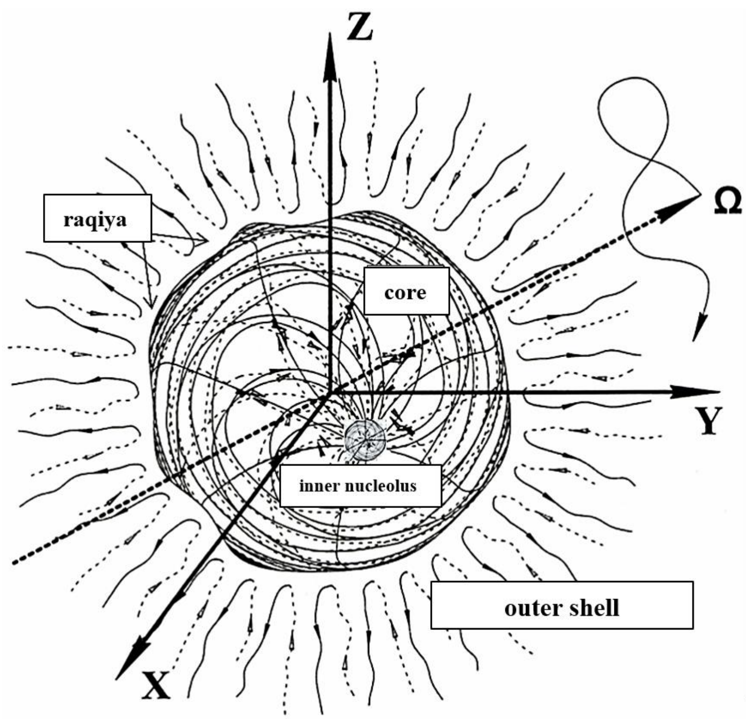

Fig. 4. A fully geometrized model of a convex stable spherical vacuum formation
(in particular, a planetary *Pe*$_y^+$-"quark$_{10}$") with four clearly defined regions:
The **core** of the planetary *Pe*$_y^+$-"quark$_{10}$" is a closed spherical region of $\lambda_{6,7}$-vacuum with a radius of $r_4 \sim 10^7$ cm = 100 km;
The **outer shell** of the *Pe*$_y^+$-"quark$_{10}$" is a region of $\lambda_{6,7}$-vacuum surrounding the core of the *Pe*$_y^+$-"quark$_{10}$";
The **raqiya** of the *Pe*$_y^+$-"quark$_{10}$" is a multilayer spherical abyss-crack separating the core of the *Pe*$_y^+$-"quark$_{10}$" from its outer shell;
The **inner nucleolus** is a closed spherical region of $\lambda_{-12,-16}$-vacuum inside the core of the *Pe*$_y^+$-"quark$_{10}$" (the core of elementary "particle");
The **substrate** *Pe*$_y^+$-"quark$_{10}$" shelf is the original undeformed region of $\lambda_{6,7}$-vacuum at the location of the *Pe*$_y^+$-"quark$_{10}$". This is a kind of memory of what this region of $\lambda_{6,7}$-vacuum was like before it was deformed and took the stable form of the *Pe*$_y^+$-"quark$_{10}$"

Similarly, in metrics (8) – (12), taking into account (19) – (22), we will also leave only those terms that contain the radii r_4. As a result, we will obtain the following multilayer metric-dynamic model of a stable "concave" spherical $\lambda_{6,7}$-vacuum formation, which we will call the valence planetary *Pe*$_y^-$-"antiquark$_{10}$".

The valence planetary Pe_y^--"ANTIQUARK$_{10}$" (35)

Stable "convex" multilayer spherical curvature of $\lambda_{6,7}$-vacuum
with signature (– + + +), consisting of:

The outer shell of the Pe_y^--«antiquark$_{10}$»
in the interval [r_3, r_4] (see negative of Figure 2*b* and 4)

I $$ds_1^{(-+++)2} = -\left(1 + \frac{r_4}{r} - \frac{r^2}{r_3^2}\right) c^2dt^2 + \frac{dr^2}{-\left(1 - \frac{r_4}{r} + \frac{r^2}{r_3^2}\right)} + r^2(d\theta^2 + sin^2\,\theta\, d\phi^2), \quad (36)$$

H $$ds_2^{(-+++)2} = -\left(1 - \frac{r_4}{r} + \frac{r^2}{r_3^2}\right) c^2dt^2 + \frac{dr^2}{-\left(1 + \frac{r_4}{r} - \frac{r^2}{3}\right)} + r^2(d\theta^2 + sin^2\,\theta\, d\phi^2), \quad (37)$$

V $$ds_3^{(-+++)2} = -\left(1 + \frac{r_4}{r} + \frac{r^2}{r_3^2}\right) c^2dt^2 + \frac{dr^2}{-\left(1 - \frac{r_4}{r} - \frac{r^2}{r_3^2}\right)} + r^2(d\theta^2 + sin^2\,\theta\, d\phi^2), \quad (38)$$

H′ $$ds_4^{(-+++)2} = -\left(1 - \frac{r_4}{r} - \frac{r^2}{r_3^2}\right) c^2dt^2 + \frac{dr^2}{-\left(1 + \frac{r_4}{r} + \frac{r^2}{r_3^2}\right)} + r^2(d\theta^2 + sin^2\,\theta\, d\phi^2); \quad (39)$$

The core of the Pe_y^--"antiquark$_{10}$"
in the interval [r_4, r_5] (see negative Figure 2*b* and 4)

I $$ds_1^{(-+++)2} = -\left(1 - \frac{r_5}{r} + \frac{r^2}{r_4^2}\right) c^2dt^2 + \frac{dr^2}{\left(1 - \frac{r_5}{r} + \frac{r^2}{r_4^2}\right)} + r^2(d\theta^2 + sin^2\,\theta\, d\phi^2), \quad (40)$$

H $$ds_2^{(-+++)2} = -\left(1 + \frac{r_5}{r} - \frac{r^2}{r_4^2}\right) c^2dt^2 + \frac{dr^2}{\left(1 + \frac{r_5}{r} - \frac{r^2}{r_4^2}\right)} + r^2(d\theta^2 + sin^2\,\theta\, d\phi^2), \quad (41)$$

V $$ds_3^{(-+++)2} = -\left(1 - \frac{r_5}{r} - \frac{r^2}{r_4^2}\right) c^2dt^2 + \frac{dr^2}{\left(1 - \frac{r_5}{r} - \frac{r^2}{r_4^2}\right)} + r^2(d\theta^2 + sin^2\,\theta\, d\phi^2), \quad (42)$$

H′ $$ds_4^{(-+++)2} = -\left(1 + \frac{r_5}{r} + \frac{r^2}{r_4^2}\right) c^2dt^2 + \frac{dr^2}{\left(1 + \frac{r_5}{r} + \frac{r^2}{r_4^2}\right)} + r^2(d\theta^2 + sin^2\,\theta\, d\phi^2); \quad (43)$$

The substrate of the Pe_y^--"antiquark$_{10}$"
in the interval [0, ∞]

i $$ds_5^{(-+++)2} = -c^2dt^2 + dr^2 + r^2(d\theta^2 + sin^2\,\theta\, d\phi^2). \quad (44)$$

Recall that according to §1 in [7], the simplest (framework) metric-dynamic models of vacuum formations are called valence, since within the framework of the Algebra of signature, each of the metrics (26) – (34) and (36) – (44) can be represented as a sum of 7 sub-metrics with the corresponding signatures (see the ranking expression (23) in [7]), and this can continue ad infinitum. That is, all the vacuum formations under consideration are infinitely complex. We simplify complex vacuum fluctuations using averaging (see Figure 2 in [7]), as a result we reveal the main framework of the vacuum formation, and the model of the simplified formation is called *valence*.

The sets of metrics (25) and (35) differ only in signature. That is, the planetary Pe_y^+-"quark$_{10}$" and the planetary Pe_y^--"antiquark$_{10}$" are completely identical, but antipodal (mutually opposite) copies of each other. If Pe_y^+-"quark$_{10}$" is conventionally called a «convex» stable spherical $\lambda_{6,7}$-vacuum formation (see Figures 2*b* and 4), then Pe_y^--"antiquark$_{10}$" is exactly the same conventionally «concave» stable spherical $\lambda_{6,7}$-vacuum formation. Such a mutually opposite pair of $\lambda_{6,7}$-vacuum formations completely corresponds to the condition of vacuum balance (see the Introduction in [1]).

The analysis of the sets of metrics-solution (25) and (35) using the mathematical apparatus of Algebra of signature [1,2,3,4,5,6] was performed in [7]. That is, everything that was presented in the article [7] is applicable to this article, provided that all triples of radii r_5, r_6, r_7 are replaced by triples of radii r_3, r_4, r_5, where all r_3, r_4, r_5, r_6, r_7 belong to the same hierarchy of radii (24) (or (44a) in [6]).

3 Naked planetary valence P_k-«quarks$_3$»

When considering the hierarchical cosmological model proposed in [6], we came to the conclusion (see §6 in [6]) that any variants of hierarchical chains of stable spherical vacuum formations with cores radii from the hierarchical series are possible: $r_1 \sim 10^{39}$, $r_2 \sim 10^{29}$, $r_3 \sim 10^{19}$, $r_4 \sim 10^{7}$, $r_5 \sim 10^{-3}$, $r_6 \sim 10^{-13}$, $r_7 \sim 10^{-24}$, $r_8 \sim 10^{-34}$, $r_9 \sim 10^{-45}$, $r_9 \sim 10^{-55}$, … (see the set of vacuum equations (169) in [6]).

We do not know which radius in this hierarchical chain is the largest and which is the smallest. We have conditionally accepted that the largest is the radius of the mega-Universe $r_1 \sim 10^{39}$ cm, and the smallest is the radius of the instanton $r_{10} \sim 10^{-55}$ cm. However, as shown in [6], the hierarchical cosmological model clearly dictates the necessity that all hierarchical chains of corpuscles nested inside each other must begin with the largest corpuscle and end with the smallest corpuscle, regardless of the number of links (i.e. intermediate corpuscles) in these hierarchical chains.

Therefore, the shortest hierarchical chain can consist of at least 3 links (corpuscles). In relation to the planetary level of stable $\lambda_{6,7}$-vacuum formations considered here, the simplest metric-dynamic model of a planetary P_k-"quarks$_3$" and P_k-"antiquarks$_3$" consists of three corpuscles: the largest, planetary, and smallest:

The valence planetary P_{ey}^+-"QUARK$_3$" (45)

Stable "convex" multilayer spherical curvature of $\lambda_{6,7}$-vacuum
with signature (+ – – –), consisting of:

The outer shell of the Pe_y^+-"quark$_3$"
in the interval $[r_1, r_4]$ (see Figure 2*b* and 4)

$$ds_1^{(+---)2} = \left(1 - \frac{r_4}{r} + \frac{r^2}{r_1^2}\right) c^2dt^2 - \frac{dr^2}{\left(1 - \frac{r_4}{r} + \frac{r^2}{r_1^2}\right)} - r^2(d\theta^2 + sin^2\,\theta\, d\phi^2), \tag{46}$$

$$ds_2^{(+---)2} = \left(1 + \frac{r_4}{r} - \frac{r^2}{r_1^2}\right) c^2dt^2 - \frac{dr^2}{\left(1 + \frac{r_4}{r} - \frac{r^2}{r_1^2}\right)} - r^2(d\theta^2 + sin^2\,\theta\, d\phi^2), \tag{47}$$

$$ds_3^{(+---)2} = \left(1 - \frac{r_4}{r} - \frac{r^2}{r_1^2}\right) c^2dt^2 - \frac{dr^2}{\left(1 - \frac{r_4}{r} - \frac{r^2}{r_1^2}\right)} - r^2(d\theta^2 + sin^2\,\theta\, d\phi^2), \tag{48}$$

$$ds_4^{(+---)2} = \left(1 + \frac{r_4}{r} + \frac{r^2}{r_1^2}\right) c^2dt^2 - \frac{dr^2}{\left(1 + \frac{r_4}{r} + \frac{r^2}{r_1^2}\right)} - r^2(d\theta^2 + sin^2\,\theta\, d\phi^2); \tag{49}$$

The core of the Pe_y^+-"quark$_3$"
in the interval $[r_4, r_{10}]$ (see Figure 2*b* and 4)

$$ds_1^{(+---)2} = -\left(1 - \frac{r_{10}}{r} + \frac{r^2}{r_4^2}\right) c^2dt^2 - \frac{dr^2}{-\left(1 - \frac{r_{10}}{r} + \frac{r^2}{r_4^2}\right)} - r^2(d\theta^2 + sin^2\,\theta\, d\phi^2), \tag{50}$$

$$ds_2^{(+---)2} = -\left(1 + \frac{r_{10}}{r} - \frac{r^2}{r_4^2}\right) c^2dt^2 - \frac{dr^2}{-\left(1 + \frac{r_{10}}{r} - \frac{r^2}{r_4^2}\right)} - r^2(d\theta^2 + sin^2\,\theta\, d\phi^2), \tag{51}$$

$$ds_3^{(+---)2} = -\left(1 - \frac{r_{10}}{r} - \frac{r^2}{r_4^2}\right) c^2dt^2 - \frac{dr^2}{-\left(1 - \frac{r_{10}}{r} - \frac{r^2}{r_4^2}\right)} - r^2(d\theta^2 + sin^2\,\theta\, d\phi^2), \tag{52}$$

$$ds_4^{(+---)2} = -\left(1 + \frac{r_{10}}{r} + \frac{r^2}{r_4^2}\right) c^2dt^2 - \frac{dr^2}{-\left(1 + \frac{r_{10}}{r} + \frac{r^2}{r_4^2}\right)} - r^2(d\theta^2 + sin^2\,\theta\, d\phi^2); \tag{53}$$

The substrate of the Pe_y^+-"quark$_3$"
in the interval $[0, \infty]$

$$ds_5^{(+---)2} = c^2dt^2 - dr^2 - r^2(d\theta^2 + sin^2\,\theta\, d\phi^2). \tag{54}$$

The valence planetary $P_{e\text{y}}^{-}$-"ANTIQUARK$_{10}$" (55)

Stable "convex" multilayer spherical curvature of $\lambda_{6,7}$-vacuum
with signature (– + + +), consisting of:

The outer shell of the Pe_{y}^{-}-"antiquark$_3$"

in the interval [r_1, r_4] (see negative of Figure 2*b* and 4)

$$ds_1^{(-+++)2} = -\left(1+\frac{r_4}{r}-\frac{r^2}{r_1^2}\right)c^2dt^2 + \frac{dr^2}{-\left(1-\frac{r_4}{r}+\frac{r^2}{r_1^2}\right)} + r^2(d\theta^2 + sin^2\,\theta\, d\phi^2), \quad (56)$$

$$ds_2^{(-+++)2} = -\left(1-\frac{r_4}{r}+\frac{r^2}{r_1^2}\right)c^2dt^2 + \frac{dr^2}{-\left(1+\frac{r_4}{r}-\frac{r^2}{1}\right)} + r^2(d\theta^2 + sin^2\,\theta\, d\phi^2), \quad (57)$$

$$ds_3^{(-+++)2} = -\left(1+\frac{r_4}{r}+\frac{r^2}{r_1^2}\right)c^2dt^2 + \frac{dr^2}{-\left(1-\frac{r_4}{r}-\frac{r^2}{r_1^2}\right)} + r^2(d\theta^2 + sin^2\,\theta\, d\phi^2), \quad (58)$$

$$ds_4^{(-+++)2} = -\left(1-\frac{r_4}{r}-\frac{r^2}{r_1^2}\right)c^2dt^2 + \frac{dr^2}{-\left(1+\frac{r_4}{r}+\frac{r^2}{r_1^2}\right)} + r^2(d\theta^2 + sin^2\,\theta\, d\phi^2); \quad (59)$$

The core of the Pe_{y}^{-}-"antiquark$_3$"

in the interval [r_4, r_{10}] (see negative Figure 2*b* and 4)

$$ds_1^{(-+++)2} = -\left(1-\frac{r_{10}}{r}+\frac{r^2}{r_4^2}\right)c^2dt^2 + \frac{dr^2}{\left(1-\frac{r_{10}}{r}+\frac{r^2}{r_4^2}\right)} + r^2(d\theta^2 + sin^2\,\theta\, d\phi^2), \quad (60)$$

$$ds_2^{(-+++)2} = -\left(1+\frac{r_{10}}{r}-\frac{r^2}{r_4^2}\right)c^2dt^2 + \frac{dr^2}{\left(1+\frac{r_{10}}{r}-\frac{r^2}{r_4^2}\right)} + r^2(d\theta^2 + sin^2\,\theta\, d\phi^2), \quad (61)$$

$$ds_3^{(-+++)2} = -\left(1-\frac{r_{10}}{r}-\frac{r^2}{r_4^2}\right)c^2dt^2 + \frac{dr^2}{\left(1-\frac{r_{10}}{r}-\frac{r^2}{r_4^2}\right)} + r^2(d\theta^2 + sin^2\,\theta\, d\phi^2), \quad (62)$$

$$ds_4^{(-+++)2} = -\left(1+\frac{r_{10}}{r}+\frac{r^2}{r_4^2}\right)c^2dt^2 + \frac{dr^2}{\left(1+\frac{r_{10}}{r}+\frac{r^2}{r_4^2}\right)} + r^2(d\theta^2 + sin^2\,\theta\, d\phi^2); \quad (63)$$

The substrate of the Pe_{y}^{-}-"antiquark$_3$"

in the interval [0, ∞]

$$ds_5^{(-+++)2} = -c^2dt^2 + dr^2 + r^2(d\theta^2 + sin^2\,\theta\, d\phi^2). \quad (64)$$

где согласно иерархии радиусов (24):

$r_1 \sim 10^{39}$ cm is radius commensurate with the radius of the mega-Universe core;
$r_4 \sim 10^{7}$ cm is radius commensurate with the radius of the core of a P_k-"quark$_3$" or P_k-"antiquark$_3$";
$r_{10} \sim 10^{-55}$ cm is radius commensurate with the size of the instanton core.

Let's note once again that the maximum radius of the core of our Universe $r_1 \sim 10^{39}$ cm, and the radius of the core of the smallest corpuscle $r_{10} \sim 10^{-55}$ cm are accepted conditionally (heuristically). However, at this stage of research, these assumptions have practically no effect on the metric-dynamic models of naked P_k-"quark$_3$" (45) and P_k-"antiquark$_3$" (55). These models of naked P_k-"quarks$_3$" can always be corrected by specifying the values of the radii r_1, r_4, r_{10}.

Naked planetary P_k-"quark$_3$" and P_k-"quark$_{10}$", as well as naked planetary P_k-"antiquark$_3$" and P_k-"antiquark$_{10}$" are practically indistinguishable at a large distance from the periphery of their cores. However, in the vicinity of their cores (i.e. in the region of their raqiya, see Figure 4) they differ significantly from each other (see §4.11 in [6] and §6 in [7]).

Planetary P_k-"quarks$_3$" (as well as "quarks" of any level of consideration, for example, the level of elementary "particles" [6,7]) have individual features in the raqiya region, depending on which hierarchical chain of stable $\lambda_{m,n}$-vacuum formations they are included in and what place they occupy in this hierarchy.

The valence planetary Pe_y^+-"quark$_3$" of the type (25) or (45) will also be called the valence planetary P_k-"electron$_3$", and the valence planetary Pe_y^--"antiquark$_3$" of the type (35) or (55) will be called the valence planetary P_k-"positron$_3$".

The metric-dynamic models of the naked valence planetary P_k-"electron$_3$" (25) or (45) and the naked valence planetary P_k-"positron$_3$" (35) or (55) almost completely coincide with the metric-dynamic models of the «electron» (50) in [7] and the "positron" (60) in [7], which were investigated in [7]. These macro- and picoscopic stable spherical $\lambda_{m,n}$-vacuum formations (corpuscles) differ mainly in scale, with the exception of raqiya. The sizes of planetary corpuscles are approximately 20 orders of magnitude larger than the sizes of elementary "particles", however, all $\lambda_{m,n}$-vacuum formations, regardless of their scale, are investigated by the same methods proposed in [1,2,3,4,5,6,7,8,9].

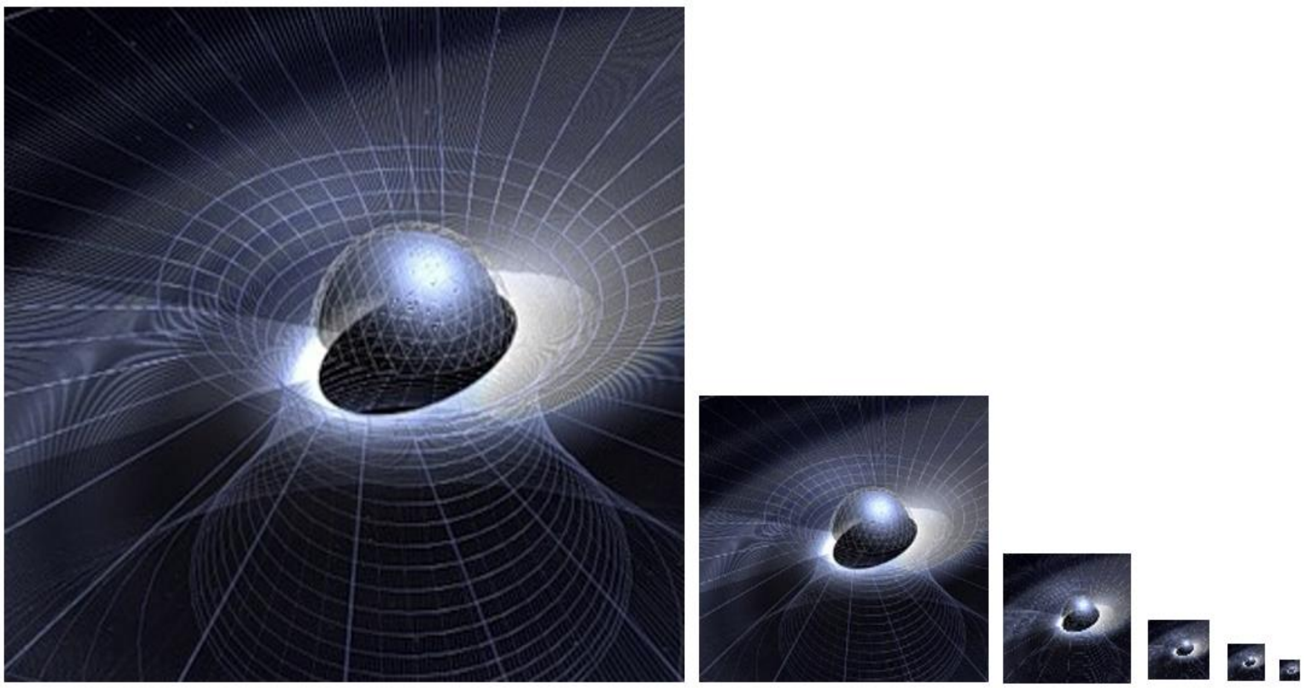

Fig. 5. Hierarchy of stable spherical $\lambda_{m,n}$-vacuum formations (corpuscles)

4 Naked colored planetary valence P_k-"quarks$_3$"

In the articles [1,2,3,4,5,6,7], where «Geometrized vacuum physics from the standpoint of the Algebra of signature» is consistently developed, it is shown that it is necessary to take into account all 16 signatures:

$$\begin{array}{cccc}
(++++) & (+++-) & (-++-) & (++-+) \\
(---+) & (-+++) & (--++) & (-+-+) \\
(+--+) & (++--) & (+---) & (+-++) \\
(--+-) & (+-+-) & (-+--) & (----)
\end{array} \qquad (65)$$

Therefore, by analogy with Table 1 in [6], we introduce the concept of convex-concave $\lambda_{6,7}$-vacuum formations, which we will call colored naked valence planetary P_k-"quarks$_3$".

Table 1 – Colored naked valence planetary P_k-"quarks$_3$"

Signature type, i.e. number of + and –	$\boldsymbol{P_k}$-"**quarks**$_3$"		$\boldsymbol{P_k}$-"**antiquarks**$_3$"		Color $\boldsymbol{P_k}$-"**quark**$_3$" or $\boldsymbol{P_k}$-"**antiquark**$_3$"
	10 metrics of the type (45) with signature:	Designation $\boldsymbol{P_k}^+$-"**quark**$_3$" naked, valent	10 metrics of the type (55) with signature:	Designation $\boldsymbol{P_k}^-$-"**antiquark**$_3$" naked, valent	
1–3	(+ – – –)	Pe_y^+-"quark$_3$" (or P_k-"electron$_3$")	(– + + +)	Pe_y^--"antiquark$_3$" (or P_k^+-"positron$_3$")	yellow
1–3	(+ + + –)	Pd_r^+-"quark$_3$"	(– – – +)	Pd_r^--"antiquark$_3$"	red
	(+ + – +)	Pd_g^+-"quark$_3$"	(– – + –)	Pd_g^--"antiquark$_3$"	green
	(+ – + +)	Pd_b^+-"quark$_3$"	(– + – –)	Pd_b^--"antiquark$_3$"	blue
2–2	(+ – – +)	Pu_r^+-"quark$_3$"	(– + + –)	Pu_r^--"antiquark$_3$"	red
	(+ – + –)	Pu_g^+-"quark$_3$"	(– + – +)	Pu_g^--"antiquark$_3$"	green
	(+ + – –)	Pu_b^+-"quark$_3$"	(– – + +)	Pu_b^--"antiquark$_3$"	blue
4	(+ + + +)	Pi_w^+-"quark$_3$"	(– – – –)	Pi_w^--"antiquark$_3$"	white

Для примера, представим $Pu_к^-$-«антикварк$_3$» в развернутом виде:

The valence planetary $\boldsymbol{Pu_r^-}$-"ANTIQUARK$_3$" (66)

Stable "convex" multilayer spherical curvature of $\lambda_{6,7}$-vacuum
with signature (– + + –), consisting of:

The outer shell of the $\boldsymbol{Pu_r^-}$-"antiquark$_3$"
in the interval [r_1, r_4]

$$ds_1^{(-++-)2} = -\left(1-\frac{r_4}{r}+\frac{r^2}{r_1^2}\right)c^2dt^2 + \frac{dr^2}{\left(1-\frac{r_4}{r}+\frac{r^2}{r_1^2}\right)} + r^2d\theta^2 - r^2sin^2\,\theta\,d\phi^2, \tag{67}$$

$$ds_2^{(-++-)2} = -\left(1+\frac{r_4}{r}-\frac{r^2}{r_5^2}\right)c^2dt^2 + \frac{dr^2}{\left(1+\frac{r_4}{r}-\frac{r^2}{r_1^2}\right)} + r^2d\theta^2 - r^2sin^2\,\theta\,d\phi^2, \tag{68}$$

$$ds_3^{(-++-)2} = -\left(1-\frac{r_4}{r}-\frac{r^2}{r_5^2}\right)c^2dt^2 + \frac{dr^2}{\left(1-\frac{r_4}{r}-\frac{r^2}{r_1^2}\right)} + r^2d\theta^2 - r^2sin^2\,\theta\,d\phi^2, \tag{69}$$

$$ds_4^{(-++-)2} = -\left(1+\frac{r_4}{r}+\frac{r^2}{r_5^2}\right)c^2dt^2 + \frac{dr^2}{\left(1+\frac{r_4}{r}+\frac{r^2}{r_1^2}\right)} + r^2d\theta^2 - r^2sin^2\,\theta\,d\phi^2; \tag{70}$$

The core of the Pu_r^--"antiquark$_3$"
in the interval [r_4, r_{10}]

$$ds_1^{(-++-)2} = -\left(1-\frac{r_{10}}{r}+\frac{r^2}{r_4^2}\right)c^2dt^2+\frac{dr^2}{\left(1-\frac{r_{10}}{r}+\frac{r^2}{r_4^2}\right)}+r^2d\theta^2-r^2sin^2\,\theta\,d\phi^2 \quad (71)$$

$$ds_2^{(-++-)2} = -\left(1+\frac{r_{10}}{r}-\frac{r^2}{r_4^2}\right)c^2dt^2+\frac{dr^2}{\left(1+\frac{r_{10}}{r}-\frac{r^2}{r_4^2}\right)}+r^2d\theta^2-r^2sin^2\,\theta\,d\phi^2, \quad (72)$$

$$ds_3^{(-++-)2} = -\left(1-\frac{r_{10}}{r}-\frac{r^2}{r_4^2}\right)c^2dt^2+\frac{dr^2}{\left(1-\frac{r_{10}}{r}-\frac{r^2}{r_4^2}\right)}+r^2d\theta^2-r^2sin^2\,\theta\,d\phi^2, \quad (73)$$

$$ds_4^{(-++-)2} = -\left(1+\frac{r_{10}}{r}+\frac{r^2}{r_4^2}\right)c^2dt^2+\frac{dr^2}{\left(1+\frac{r_{10}}{r}+\frac{r^2}{r_4^2}\right)}+r^2d\theta^2-r^2sin^2\,\theta\,d\phi^2; \quad (74)$$

The substrate of the Pu_r^--"antiquark$_3$"
in the interval [0, ∞]

$$ds_5^{(-++-)2} = -c^2dt^2+dr^2+r^2d\theta^2-r^2sin^2\,\theta\,d\phi^2. \quad (75)$$

The metric-dynamic models of all other P_k-"quarks$_3$" and P_k-"antiquarks$_3$" listed in Table 1 are based on a set of metrics of the form (67) – (75), but with the corresponding signature.

Except for the on-average convex planetary P_k-"electron$_3$" (i.e., Pe_y^+-"quark$_3$") with the signature (+ – – –) and the on-average concave planetary P_k-"positron$_3$" (i.e., Pe_y^--"antiquark$_3$") with the signature (– + + +), all other planetary P_k-"quarks$_3$" are unstable convex-concave curvatures of the $\lambda_{6,7}$-vacuum, since all metrics, for example, of the form (67) – (75) with the signature (– + + –), are not solutions of the Einstein vacuum equation (2). That is, when substituting the components of metric tensors from metrics of the form (67) – (74), with any other signature except (+ – – –) and (– + + +), into Einstein's second vacuum equation (2), equality to zero does not occur.

5 Naked valence planetary P_k-"baryons$_3$", P_k-"mesons$_3$", P_k-"bosons$_3$" and P_k-"atoms$_3$"

5 naked, valence planetary P_k-"baryons$_3$", P_k-"mesons$_3$", P_k-"bosons$_3$" and P_k-"atoms$_3$"

Similarly, to how it was done in §§4.3 – 4.7 in [6] for the level of elementary "particles", from the set of 16-color naked valence planetary P_k-"quarks$_3$" and P_k-"antiquarks$_3$" the following can be composed:

- three states of the naked valence planetary Pp_i^--"proton$_3$" (i = 1, 2, 3) with the total signature (– + + +):

$$\begin{array}{ll} Pd_r^+(+\;+\;+\;-) & \\ Pu_g^-(-\;+\;-\;+) & (76)\\ Pu_b^-\underline{(-\;-\;+\;+)} & \\ Pp_1^-(-\;+\;+\;+)_+ & \end{array} \qquad \begin{array}{ll} Pd_g^+(+\;+\;-\;+) & \\ Pu_g^-(-\;-\;+\;+) & (77)\\ Pu_r^-\underline{(-\;+\;+\;-)} & \\ Pp_2^-(-\;+\;+\;+)_+ & \end{array} \qquad \begin{array}{ll} Pd_b^+(+\;-\;+\;+) & \\ Pu_r^-(-\;+\;+\;-) & (78)\\ Pu_g^-\underline{(-\;+\;-\;+)} & \\ Pp_3^-(-\;+\;+\;+)_+ & \end{array}$$

- three states of the naked valence planetary Pp_i^+-"antiproton$_3$" with the total signature (+ – – –):

$$\begin{array}{ll} Pd_r^-(-\;-\;-\;+) & \\ Pu_g^+(+\;-\;+\;-) & (79)\\ Pu_b^+\underline{(+\;+\;-\;-)} & \\ Pp_1^+(+\;-\;-\;-)_+ & \end{array} \qquad \begin{array}{ll} Pd_g^-(-\;-\;+\;-) & \\ Pu_b^+(+\;+\;-\;-) & (80)\\ Pu_r^+\underline{(+\;-\;-\;+)} & \\ Pp_2^+(+\;-\;-\;-)_+ & \end{array} \qquad \begin{array}{ll} Pd_g^-(-\;+\;-\;-) & \\ Pu_r^+(+\;-\;-\;+) & (81)\\ Pu_g^+\underline{(+\;-\;+\;-)} & \\ Pp_3^+(+\;-\;-\;-)_+ & \end{array}$$

see §4.3 in [6];

- eight states of the naked valence planetary Pn_i^0-"neutron$_3$" (where i = 1,..,8) with the total signature (0 0 0 0) (§4.4 in [6]):

(82)

$$\begin{array}{llll}
Pi_w^-\ (-\ -\ -\ -) & Pi_w^-\ (-\ -\ -\ -) & Pi_w^-\ (-\ -\ -\ -) & Pi_w^-\ (-\ -\ -\ -) \\
Pd_b^+\ (+\ -\ +\ +) & Pd_g^+\ (+\ +\ -\ +) & Pd_b^+\ (+\ -\ +\ +) & Pu_g^-\ (-\ +\ -\ +) \\
Pu_r^-\ (-\ +\ +\ -) & Pd_r^+\ (+\ +\ +\ -) & Pu_g^-\ (-\ +\ -\ +) & Pd_b^+\ (+\ -\ +\ +) \\
Pd_g^+\ \underline{(+\ +\ -\ +)} & Pu_b^-\ \underline{(-\ -\ +\ +)} & Pd_r^+\ \underline{(+\ +\ +\ -)} & Pd_r^+\ \underline{(+\ +\ +\ -)} \\
Pn_1^0\ (0\ 0\ 0\ 0)_+ & Pn_2^0\ (0\ 0\ 0\ 0)_+ & Pn_3^0\ (0\ 0\ 0\ 0)_+ & Pn_4^0\ (0\ 0\ 0\ 0)_+
\end{array}$$

$$\begin{array}{llll}
Pi_w^+\ (+\ +\ +\ +) & Pi_w^+\ (+\ +\ +\ +) & Pi_w^+\ (+\ +\ +\ +) & Pi_w^+\ (+\ +\ +\ +) \\
Pd_b^-\ (-\ +\ -\ -) & Pd_g^-\ (-\ -\ +\ -) & Pd_b^-\ (-\ +\ -\ -) & Pu_g^+\ (+\ -\ +\ -) \\
Pu_r^+\ (+\ -\ -\ +) & Pd_r^-\ (-\ -\ -\ +) & Pu_g^+\ (+\ -\ +\ -) & Pd_b^-\ (-\ +\ -\ -) \\
Pd_g^-\ \underline{(-\ -\ +\ -)} & Pu_b^+\ \underline{(+\ +\ -\ -)} & Pd_r^-\ \underline{(-\ -\ -\ +)} & Pd_r^-\ \underline{(-\ -\ -\ +)} \\
Pn_5^0\ (0\ 0\ 0\ 0)_+ & Pn_6^0\ (0\ 0\ 0\ 0)_+ & Pn_7^0\ (0\ 0\ 0\ 0)_+ & Pn_8^0\ (0\ 0\ 0\ 0)_+
\end{array}$$

- all naked valence planetary Pm_i^--"mesons$_3$". For example, a naked valence planetary $P\pi^+$-"meson$_3$" ($P\pi^+ = Pu^-Pd^+$)

(83)

$$\begin{array}{lll}
Pd_r^+\ (+\ +\ +\ -) & Pd_g^+\ (+\ +\ -\ +) & Pd_b^+\ (+\ -\ +\ +) \\
P\underline{u_g^-\ (-\ +\ -\ +)} & P\underline{u_b^-\ (-\ -\ +\ +)} & P\underline{u_r^-\ (-\ +\ +\ -)} \\
P\pi_1^+\ (0\ 2+\ 0\ 0)_+ & P\pi_2^+\ (0\ 0\ 0\ 2+)_+ & P\pi_3^+\ (0\ 0\ 2+\ 0)_+
\end{array}$$

or a naked valence planetary $P\pi^0$-"meson$_3$" $\{P\pi^0 = \frac{1}{\sqrt{2}}(Pu^-Pu^+ - Pd^+Pd^-)\}$ (see §4.7 in [6])

(84)

$$\begin{array}{lll}
Pu_r^+\ (+\ -\ -\ +) & Pu_g^+\ (+\ -\ +\ -) & Pu_b^+\ (+\ +\ -\ -) \\
Pu_g^-\ (-\ +\ -\ +) & Pu_b^-\ (-\ -\ +\ +) & Pu_r^-\ (-\ +\ +\ -) \\
- & - & - \\
Pd_r^+\ (+\ +\ +\ -) & Pd_g^+\ (+\ +\ -\ +) & Pd_b^+\ (+\ -\ +\ +) \\
P\underline{d_g^-\ (-\ -\ +\ -)} & P\underline{d_b^-\ (-\ +\ -\ -)} & P\underline{d_r^-\ (-\ -\ -\ +)} \\
P\pi_1^0\ (0\ 0\ 0\ 0)_+ & P\pi_2^0\ (0\ 0\ 0\ 0)_+ & P\pi_3^0\ (0\ 0\ 0\ 0)_+
\end{array}$$

- all naked valence planetary P_k-"atoms$_3$". For example, all states of the naked valence planetary P_{H2}-"deuterium$_3$"

(85)

$$\begin{array}{llllll}
 & (+\ +\ +\ -) & & (+\ +\ -\ +) & & \\
Pp^-\text{-"proton}_3\text{"} & (-\ +\ -\ +) & & (-\ -\ +\ +) & & \\
 & (-\ -\ +\ +) & & (-\ +\ +\ -) & & \\
+ & (-\ -\ -\ -) & & (+\ +\ +\ +) & & \\
Pn^0\text{-"neutron}_3\text{"} & (+\ -\ +\ +) & \text{or} & (+\ -\ +\ -) & \text{or} & \ldots \\
+ & (-\ +\ +\ -) & & (-\ +\ -\ -) & & \\
 & (+\ +\ -\ +) & & (-\ -\ -\ +) & & \\
\underline{Pe^+\text{-"electron}_3\text{"}} & \underline{(+\ -\ -\ -)} & & \underline{(+\ -\ -\ -)} & & \\
P_{H2}\text{-"deuterium}_3\text{"} & P_{H2}(0\ 0\ 0\ 0)_+ & & P_{H2}(0\ 0\ 0\ 0)_+ & &
\end{array}$$

(86)

$$\begin{array}{llllll}
 & (-\ -\ -\ +) & & (-\ -\ +\ -) & & \\
Pp^+\text{-"antiproton}_3\text{"} & (+\ -\ +\ -) & & (+\ +\ -\ -) & & \\
 & (+\ +\ -\ -) & & (+\ -\ -\ +) & & \\
+ & (+\ +\ +\ +) & & (-\ -\ -\ -) & & \\
Pn^0\text{-"neutron}_3\text{"} & (-\ +\ -\ -) & \text{or} & (-\ +\ -\ +) & \text{or} & \ldots \\
+ & (+\ -\ -\ +) & & (+\ -\ +\ +) & & \\
 & (-\ -\ +\ -) & & (+\ +\ +\ -) & & \\
\underline{Pe^-\text{-"positron}_3\text{"}} & \underline{(-\ +\ +\ +)} & & \underline{(-\ +\ +\ +)} & & \\
P_{H2}\text{-"deuterium}_3\text{"} & P_{H2}(0\ 0\ 0\ 0)_+ & & P_{H2}(0\ 0\ 0\ 0)_+ & &
\end{array}$$

where each signature corresponds to a planetary P_k-"quark$_3$" from Table 1, i.e. a set of 10 metrics of type (66) with the corresponding signature. See §4.5 in [6].

Or, for example, one of the many nodal (topological) configurations of the planetary valence P_k-"atom$_3$" of helium (or P_{He4}-"helium$_3$"), see §4.6 in [6]:

$$
\begin{array}{cl}
\begin{matrix}(+ & + & - & +)\\(- & - & + & +)\\(- & + & + & -)\end{matrix} & \text{the planetary } Pp_2^{-}\text{-"proton}_3\text{"}\\[2ex]
\begin{matrix}(- & + & - & -)\\(+ & - & - & +)\\(+ & - & + & -)\end{matrix} & \text{the planetary } Pp_3^{+}\text{-"antiproton}_3\text{"}\\[2ex]
(- \;\; + \;\; + \;\; +) & \text{the planetary } P_{e}^{-}\text{-"positron}_3\text{"}\\[2ex]
\begin{matrix}(- & - & - & -)\\(+ & + & - & +)\\(+ & + & + & -)\\(- & - & + & +)\end{matrix} & \text{the planetary } Pn_2^{0}\text{-"neutron}_3\text{"}\\[2ex]
\begin{matrix}(+ & + & + & +)\\(+ & - & + & -)\\(- & + & - & -)\\(- & - & - & +)\end{matrix} & \text{the planetary } Pn_8^{0}\text{-"neutron}_3\text{"}\\[2ex]
(+ \;\; - \;\; - \;\; -) & \text{the planetary } P_{e}^{-}\text{-"electron}_3\text{"}\\
\hline
P_{He4}\,(0 \;\; 0 \;\; 0 \;\; 0)_{+} & \text{the planetary } P_{He4}\text{-"helium}_3\text{".}
\end{array}
\qquad (87)
$$

Thus, from the 16-color naked planetary P_k-"quarks$_3$" from Table 1, all planetary P_k-"atoms$_3$", P_k-"molecules$_3$", P_k-"ions$_3$", etc. can be constructed.

The models of planetary P_k-"bosons$_3$" almost completely coincide with the models of picoscopic "bosons", which are presented in §4.8 in [6]. The only difference is that in all Exs. (132) – (139) in [6] it is necessary to substitute the wavelength $\lambda = \lambda_{6,7}$ from the range $\Delta\lambda = 10^6 – 10^7$ cm = 10 – 100 km.

6 The naked "Solar System$_3$"

Let's consider the naked planetary stable spherical $\lambda_{6,7}$-vacuum formations (i.e. P_k-"planets$_3$") using the example of the "Solar system", which has been studied the most.

6.1 Brief information about the Solar System

The author is not an expert in the structure of the Solar System, so inaccuracies are possible, which, however, do not affect the generality of the conclusions.

It is believed that the Solar System includes many celestial bodies (or astronomical objects): one star (the Sun), 11 planets (see Figure 6), many satellites of these planets: moons, asteroids (see Appendix 1), meteorites, comets, etc.

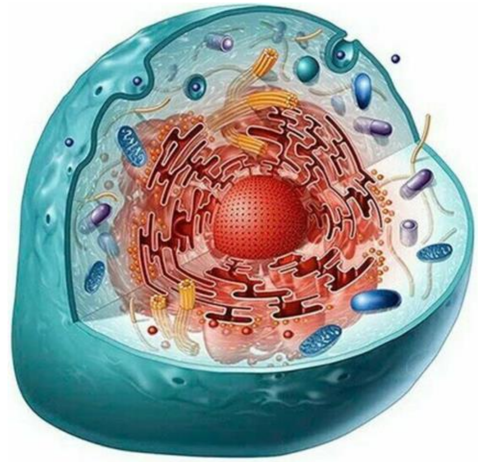

Fig. 6. Solar System **Fig. 7.** Biological cell

It is natural to assume that the naked P_k-"planets$_3$" (i.e. funnel-shaped spherical curvatures of the $\lambda_{6,7}$-vacuum, see Figures 2b and 3), considered in this article, are located only inside of a spherical celestial material bodies (i.e. inside a material star, material planets and moons). This assumption is due to the belief that only a spherical curvature of the $\lambda_{6,7}$-vacuum (essentially a spherically symmetric gravitational field of a naked P_k-"planets$_3$") is capable of gathering around itself a huge accumulation of pico- and nanoscopic "particles" ("atoms" and "molecules") in the form of a regular spherical shape.

The causes of the emergence of the gravitational field in the outer shell of naked P_k-"stars$_3$" and P_k-"planets$_3$" will be (*Be Ezrat ASHEM*) considered in the next (11th) work of this series of articles under the general title «Geometrized Vacuum Physics Based on the Algebra of Signatures».

The remaining celestial bodies (asteroids, comets, meteorites, etc.) also consist of many pico- and nanoscopic "atoms" and "molecules", but they are held together not by planetary gravity, but by geometrized electromagnetic physical-chemical bonds (considered in §2 in [7] and in [8]). Therefore, as a rule, such natural astronomical objects have an irregular shape.

In that article an attempt was made to estimate the number of planetary P_k-"quarks$_3$" in the cores of a naked P_k-"star$_3$" and P_k-"planets$_3$" of the Solar System. For this purpose, we use an analogue of the phenomenological Ex. (112) in [6]

$$r_{cP} \approx ½ A^{1/3} r_4 \approx ½ A^{1/3} \cdot 10^7 \text{ cm} = ½ A^{1/3} \cdot 100 \text{ km}, \quad (88)$$

which allows us to estimate the radius of the core of a planetary vacuum formation (i.e. P_k-"planet$_3$") from the number of naked P_k-"quarks$_3$" A contained in it.

6.2 The smallest naked P_k-"planet$_3$"

We know well that in the "Solar System" there are no planetary P_k-"electrons$_3$" (45) and P_k-"positrons$_3$" (55), as well as planetary P_k-"protons$_3$" (76) – (78) and P_k-"antiprotons$_3$" (79) – (81), since these stable vacuum formations have powerful geometrized planetary electric fields (see §2.2 in [7]), which are not observed in the "Solar System$_3$".

Similar to §§2 and 10 in [7], in charged planetary $\lambda_{6,7}$-vacuum formations (such as planetary P_k-"electron$_3$" or P_k-"proton$_3$" or P_k-"ion$_3$"), subcont currents of colossal intensity flow into and out of the region surrounding their core (i.e., into their raqiya) at speeds close to the speed of light.

Such powerful subcont currents are observed only in the vicinity of the core of naked G_k-"galaxies$_3$" (which are referred to in modern literature as galactic black holes). In other words, naked G_k-"galaxies$_3$" are most likely charged spherical $\lambda_{18,19}$-vacuum formations of the galactic type: G_k-"electron$_3$" or G_k-"proton$_3$" or G_k-"ion$_3$".

Inside planetary spherical $\lambda_{6,7}$-vacuum formations (i.e. P_k -"planets$_3$" and P_k -"stars$_3$") such powerful subcont currents (with velocities close to the speed of light) are not observed. This is possible only if P_k -"planet$_3$" and P_k -"star$_3$" are electrically neutral $\lambda_{6,7}$-vacuum formations of the type planetary P_k -"atoms$_3$" and P_k -"molecules$_3$", in which powerful subcont currents in the outer shell compensate each other's manifestations (see §§4.4 and 4.5 in [6]).

It is possible that stable electrically charged planetary $\lambda_{6,7}$-vacuum formations exist in other star systems. It is also possible that when large P_k-"planets$_3$" and/or P_k-"stars$_3$" collide, they disintegrate (i.e. split) into, among other things, planetary P_k-"electrons$_3$", P_k-"positrons$_3$", P_k-"protons$_3$" and P_k-"antiprotons$_3$". But in the nearest Solar System that we are studying, such charged "astronomical objects" are absent. That is, all stable naked spherical $\lambda_{6,7}$-planetary vacuum formations in the "Solar System" are electrically neutral. This means that they are either naked planetary P_k-"atoms$_3$" or naked planetary P_k-"molecules$_3$".

Electrically neutral ones include the planetary P_k-"neutron$_3$" (82). But as was shown in §4.4 in [7], when the intranuclear topological (nodal) configuration changes, the planetary P_k-"neutron$_3$" can decay into a P_k-«electron$_3$» and a P_k-«proton$_3$», or into a P_k-"positron$_3$" and a P_k-"antiproton$_3$". Thus, if there were planetary P_k-"neutrons$_3$" in the "Solar System", they have decayed by our time.

Thus, we necessarily come to the conclusion that in the naked "Solar System" only naked stable spherical $\lambda_{6,7}$-vacuum formations of the P_k-«atomic$_3$» type can be present.

The simplest neutral stable spherical $\lambda_{6,7}$-vacuum formation is the planetary $P_{H1}{}^0$-"protium$_3$", which consists only of P_k-"proton$_3$" and P_k-"electron$_3$" or P_k-"antiproton$_3$" and P_k-"positron$_3$". The six possible topological (nodal) states of the planetary $P_{H1}{}^0$-"protium$_3$" (similar to the description of the "neutron" in §4.3 in [6]) are:

$$\begin{array}{l} Pd_r^{+}(+\ +\ +\ -) \\ Pu_g^{-}(-\ +\ -\ +) \\ Pu_b^{-}(-\ -\ +\ +) \\ Pe_y^{+}\underline{(+\ -\ -\ -)} \\ P_{H1}{}^{1}\,(0\ 0\ 0\ 0)_{+} \end{array} \quad \text{or} \quad \begin{array}{l} Pd_g^{+}(+\ +\ -\ +) \\ Pu_b^{-}(-\ -\ +\ +) \\ Pu_r^{-}(-\ +\ +\ -) \\ Pe_y^{+}\underline{(+\ -\ -\ -)} \\ P_{H1}{}^{2}\,(0\ 0\ 0\ 0)_{+} \end{array} \quad \text{or} \quad \begin{array}{l} Pd_b^{+}(+\ -\ +\ +) \\ Pu_r^{-}(-\ +\ +\ -) \\ Pu_g^{-}(-\ +\ -\ +) \\ Pe_y^{+}\underline{(+\ -\ -\ -)} \\ P_{H1}{}^{3}\,(0\ 0\ 0\ 0)_{+} \end{array} \tag{89}$$

$$\begin{array}{l} Pd_r^{-}(-\ -\ -\ +) \\ Pu_g^{+}(+\ -\ +\ -) \\ Pu_b^{+}(+\ +\ -\ -) \\ Pe_y^{-}\underline{(-\ +\ +\ +)} \\ P_{H1}{}^{4}\,(0\ 0\ 0\ 0)_{+} \end{array} \quad \text{or} \quad \begin{array}{l} Pd_g^{-}(-\ -\ +\ -) \\ Pu_b^{+}(+\ +\ -\ -) \\ Pu_r^{+}(+\ -\ -\ +) \\ Pe_y^{-}\underline{(-\ +\ +\ +)} \\ P_{H1}{}^{5}\,(0\ 0\ 0\ 0)_{+} \end{array} \quad \text{or} \quad \begin{array}{l} Pd_b^{-}(-\ +\ -\ -) \\ Pu_r^{+}(+\ -\ -\ +) \\ Pu_g^{+}(+\ -\ +\ -) \\ Pe_y^{-}\underline{(-\ +\ +\ +)} \\ P_{H1}{}^{6}\,(0\ 0\ 0\ 0)_{+} \end{array}$$

These states constantly flow into each other so that each of them is realized with a probability of 1/6, while the average state of $P_{H1}{}^0$-"protium$_3$" is described by the expression

$$P_{H1}{}^{0} = 1/6\,(P_{H1}{}^{1} + P_{H1}{}^{2} + P_{H1}{}^{3} + P_{H1}{}^{4} + P_{H1}{}^{5} + P_{H1}{}^{6}). \tag{90}$$

At the same time, from molecular chemistry, we know that hydrogen atoms H (more precisely, protium atoms) tend to unite into hydrogen molecules H_2. We assume that the properties of stable vacuum formations at different levels (scales) of matter organization are similar, therefore, at the planetary level, it is also most likely that inside small dense spherical planets there is a planetary $P_{H2}{}^0$-"hydrogen molecule$_3$", for example, in the state of the following topological nodes:

$$\begin{array}{lclcl}
Pd_r^+(+\ +\ +\ -) & & Pd_g^+(+\ +\ -\ +) & & \\
Pu_g^-(-\ +\ -\ +)\ \ P_k\text{-"proton}_3\text{"} & & Pu_b^-(-\ -\ +\ +)\ \ P_k\text{-"proton}_3\text{"} & & \\
Pu_b^-(-\ -\ +\ +) & & Pu_r^-(-\ +\ +\ -) & & \\
Pe_y^+(+\ -\ -\ -)\ \ Pe^+\text{-"electron}_3\text{"} & & Pe_y^+(+\ -\ -\ -)\ \ Pe^+\text{-"electron}_3\text{"} & & \\
Pd_g^-(-\ -\ +\ -) & \text{or} & Pd_r^-(-\ -\ -\ +) & \text{or} & \ldots \\
Pu_b^+(+\ +\ -\ -)\ \ P_k\text{-"антипротон}_3\text{"} & & Pu_g^+(+\ -\ +\ -)\ \ P_k\text{-"antiproton}_3\text{"} & & \\
Pu_r^+(+\ -\ -\ +) & & Pu_b^+(+\ +\ -\ -) & & \\
Pe_y^-\underline{(-\ +\ +\ +)}\ \ Pe^-\text{-"positron}_3\text{"} & & Pe_y^-\underline{(-\ +\ +\ +)}\ \ Pe^-\text{-"positron}_3\text{"} & & \\
P_{H2}^1\ (0\ \ 0\ \ 0\ \ 0)_+ & & P_{H2}^2\ (0\ \ 0\ \ 0\ \ 0)_+ & &
\end{array} \tag{91}$$

When the repetition of identical P_k-"quarks$_3$" with identical colors within one topological node is prohibited, there can be nine such topological combinations (i.e. states of P_{H2}^0-"hydrogen molecule$_3$"), therefore the planetary P_{H2}^0-"hydrogen molecule$_3$" is the result of averaging all these states

$$P_{H2}^0 = 1/9\ (P_{H2}^1 + P_{H2}^2 + P_{H2}^3 + P_{H2}^4 + P_{H2}^5 + P_{H2}^6 + P_{H2}^7 + P_{H2}^8 + P_{H2}^9). \tag{92}$$

We note once again that within the framework of Geometrized Vacuum Physics [1,2,3,4,6,7,8,9], in contrast to modern physics, there is no baryon asymmetry of matter. In particular, the planetary P_k-"hydrogen molecule$_3$" consists of P_k-"particles$_3$" and P_k-"antiparticles$_3$" (more precisely, of colored P_k-"quarks$_3$" and P_k-"antiquarks$_3$"), which in principle cannot annihilate, since they are intricately entangled in a single topological knot (i.e., they form a single extremely complex convex-concave curvature of the $\lambda_{6,7}$-vacuum). In order for these P_k-"particles$_3$" and P_k-"antiparticles$_3$" to annihilate, they must first become untangled.

Another, practically the same, simple planetary P_k-"atom$_3$" is the planetary P_k-"heavy hydrogen$_3$" (another name is P_D-"deuterium$_3$") (85) – (86):

$$\begin{array}{llclc}
 & (+\ +\ +\ -) & & (+\ +\ -\ +) & \\
Pp^-\text{-"proton}_3\text{"} & (-\ +\ -\ +) & & (-\ -\ +\ +) & \\
 & (-\ -\ +\ +) & & (-\ +\ +\ -) & \\
\quad + & (-\ -\ -\ -) & & (+\ +\ +\ +) & \\
Pn^0\text{-"neutron}_3\text{"} & (+\ -\ +\ +) & \text{or} & (+\ -\ +\ -) & \text{or} \\
 & (-\ +\ +\ -) & & (-\ +\ -\ -) & \\
\quad + & (+\ +\ -\ +) & & (-\ -\ -\ +) & \\
\underline{Pe^+\text{-"electron}_3\text{"}} & \underline{(+\ -\ -\ -)} & & \underline{(+\ -\ -\ -)} & \\
P_D^n\text{-"deuterium}_3\text{"} & P_D^1\ (0\ \ 0\ \ 0\ \ 0)_+ & & P_D^2(0\ \ 0\ \ 0\ \ 0)_+ &
\end{array} \tag{93}$$

$$\begin{array}{llclc}
 & (+\ +\ +\ -) & & (+\ +\ -\ +) & \\
Pp^-\text{-"proton}_3\text{"} & (-\ +\ -\ +) & & (-\ -\ +\ +) & \\
 & (-\ -\ +\ +) & & (-\ +\ +\ -) & \\
\quad + & (-\ -\ -\ -) & & (+\ +\ +\ +) & \\
Pn^0\text{-"neutron}_3\text{"} & (+\ -\ +\ +) & \text{or} & (+\ -\ +\ -) & \text{or}\ \ \ldots \\
\quad + & (-\ +\ +\ -) & & (-\ +\ -\ -) & \\
 & (+\ +\ -\ +) & & (-\ -\ -\ +) & \\
\underline{Pe^+\text{-"electron}_3\text{"}} & \underline{(+\ -\ -\ -)} & & \underline{(+\ -\ -\ -)} & \\
P_D^n\text{-"deuterium}_3\text{"} & P_D^3(0\ \ 0\ \ 0\ \ 0)_+ & & P_D^4(0\ \ 0\ \ 0\ \ 0)_+ &
\end{array}$$

Planetary P_D^0-"deuterium" is the result of averaging all n possible similar states (topological combinations)

$$P_{H2}^0 = 1/n\ (P_D^1 + P_D^2 + P_D^3 + P_D^4 + \ldots + P_D^n). \tag{94}$$

Planetary $P_{H2}{}^0$-"hydrogen molecule$_3$" and planetary $P_D{}^0$-"deuterium$_3$" consist of 8 P_k-"quarks$_3$", and they are apparently the most stable and, therefore, the most frequently encountered small stable electrically neutral spherical $\lambda_{6,7}$-vacuum formations.

Let's assume that the planetary $P_{H1}{}^0$-"protium$_3$" (90) is the smallest naked P_k-"planet$_3$", while, apparently, the most common small naked P_k-"planets$_3$" are the planetary $P_{H2}{}^0$-"hydrogen molecule$_3$" (92) and the planetary $P_D{}^0$-"deuterium$_3$" (94).

Now let's compare the small naked P_k-"planets$_3$" with the smallest material spherical planets of the Solar System.

6.3 Analysis of small celestial bodies of the Solar System

Appendix 1 contains an incomplete list of the largest small satellites of the planets of the Solar System, borrowed from the site "The Solar System Wiki". From this list, material astronomical objects on the border of the transition from spherical celestial bodies to irregularly shaped bodies are selected and presented in Table 2.

Table 2 - Parameters of small astronomical objects close to spherical shape

Planet / satellite material	**Average radius** approximately	**Density** approximately	**Mass** approximately	**Shape**	**Image**
Ceres, *planet, natural satellite of the Sun*	475 km	2.2 g/cm^3	9×10^{20} kg	Close to spherical shape	
Vesta, *asteroid, natural satellite of the Sun*	263 km	3.5 g/cm^3	2.6×10^{20} kg	Close to spherical shape	
Pallas, *planet, natural satellite of the Sun*	256 km	3.9 g/cm^3	2×10^{20} kg	Close to spherical shape	
Enceladus, *natural satellite of Saturn*	252 km	1.6 g/cm^3	1.08×10^{20} kg	Close to spherical shape	

Hygiea *natural satellite of the Sun*	217 km	1.9 g/cm^3	8×10^{19} kg	Close to spherical shape	
Proteus, *natural satellite of Neptune*	209 km	0.7 g/cm^3	5×10^{19} kg	Close to spherical shape	
Ilmarë, *natural satellite of a Kuiper belt planetoid*	178 km	0.6 g/cm^3	2.2×10^{19} kg	Close to spherical shape	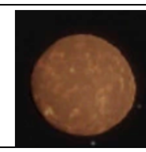
Hyperion, *natural satellite of Saturn*	135 km	0.54 g/cm^3	5.6×10^{18} kg	Irregular shape	
Phoebe, *natural satellite of Saturn*	110 km	1,6 g/cm^3	8.3×10^{18} kg	Irregular shape	
Larissa, *natural satellite of Neptune*	97 km	0.9 g/cm^3	3.72×10^{18} kg	Irregular shape	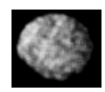

6.4 Comparison of the smallest material planets and the smallest naked P_k-"planets"

The following reasoning is preliminary and evaluative. Let's assume that inside the minimal material planet there is the smallest naked P_k-"planet" whose outer shell attracts pico-, nano- and microscopic stable $\lambda_{m,n}$-vacuum formations ("particles") by means of gravity (the nature of "planetary" gravity will be considered in the next 11th work of the proposed series of articles [1,2,3,4,5,6,7,8,9]). In this case, the more planetary P_k-"quarks$_3$" make up a naked "planet" (see, for example, ranking expression (87)), the greater the intensity of its attraction (gravity), and the more small "particles" it can attract to its core (see Figures 2*a* and 8) and hold for a long time. Therefore, the mass of a spherical planet can serve as a criterion for the intensity of gravitational attraction.

Fig. 8. Fractal illustration of the attraction of many pico-, nano- and microscopic "particles" to the core of a naked "planet" by means of the mechanism of inter-"planetary" gravity

From Table 2 it is evident that the smallest astronomical objects with a shape close to spherical are **Proteus**, **Ilmarë** and **Hygiea**. These smallest almost-spherical astronomical objects have an average radius of approximately 200 km and a mass of approximately 5×10^{19} kg. An astronomical object with such parameters will be called a minimal material planet.

It is natural to assume that inside the minimal almost-spherical material planet (with an average radius of ~ 200 km and a mass of ~ 5×10^{19} kg) there is the smallest naked P_k-"planet$_3$" (i.e. planetary $P_{H1}{}^0$-"protium$_3$" consisting of 4 P_k-"quarks$_3$" (89)).

After objects like **Proteus**, **Ilmarë** and **Hygiea**, the next largest are practically spherical astronomical objects like **Enceladus Vesta** and **Pallas** with a characteristic radius of ~ 250 km and a mass of ~ 10^{20} kg.

The third largest cosmic spherical material objects are planets like Ceres with a characteristic radius of ~ 450 km and a mass of ~ 10^{21} kg.

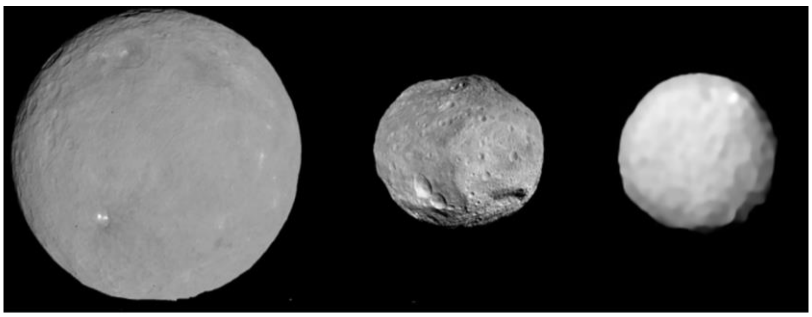

Ceres $r_{cP} \approx 475$ km | Vesta $r_{cP} \approx 263$ km | Pallas $r_{cP} \approx 256$ km

Fig. 9. Dimensions (average radii) of small astronomical objects of nearly spherical shape

Figure 9 shows an obvious partial jump from the smallest nearly spherical objects with an average radius of $r_{cP} \approx 250$ km (such as Vesta and Pallas) and an almost twice as large spherical object like Ceres with an average radius of $r_{cP} \approx$ 480 km.

To compare the parameters of material spherical astronomical objects, it is convenient to use their mass, since the mass of a planet combines its two main characteristics: dimensions (in particular, volume) and the density of matter.

Let's divide the mass of the smallest material planet (e.g. Proteus) by the mass of the material planet of the next class (e.g. Enceladus)

$10^{20} / (5\times10^{19}) = 2$.

Multiply the resulting number 2 by 4 (the minimum number of P_k-"quarks$_3$" in the smallest P_k-"atom$_3$", i.e. in the planetary $P_{H1}{}^0$-"proteus$_3$"). As a result, we get 8 – this, within the framework of the proposed methodology, means that material spherical astronomical objects of the second class of smallness (like Enceladus) contain 8 P_k-"quarks$_3$".

This logic indicates that inside the second class of small material planets there is the following quantum (in the sense of discrete) version of a naked P_k-"planet$_3$": 8-"quark$_3$" planetary $P_{H2}{}^0$-"hydrogen molecule$_3$" (91) or 8-"quark$_3$" planetary $P_D{}^0$-"deuterium$_3$" (93).

Continuing this logic, we propose to estimate the number of planetary P_k-"quarks$_3$" that make up naked "planets" located inside the material planets of the Solar System using the following method.

We divide the mass of a material planet M by the mass of the smallest material planet $m = 5\times10^{19}$ kg, and multiply the result of this division by 4 (the number of P_k-"quarks$_3$" that make up the smallest naked P_k-"planet$_3$").

The results of calculations using this method are presented in Table. 2.

Table 2 – Approximate characteristics of astronomical objects of the Solar System

Star / planet	**Radius of the material planet,** average ~ R	**Density of the material planet,** average ~ ρ	**Mass** of the material planet, ~ M	**Ratio** of the mass of the celestial body to the mass of the minimal planet ~ M/m	**Estimate of the number of** P_k-"quarks$_3$" $\frac{M}{m} \times 4$	**Radius** of the core of the naked P_k-"planet$_3$", approximately
Минимальная вещественная планета, типа Протей	200 km	1.2 g/cm^3	m= 5×10^{19}kg	1	4	100 km
Sun	696 000 km	1.41 g/cm^3	1.99×10^{30} kg	0.4×10^{11}	1.6 ×10^{11}	316 000 km
Mercury	2439.7 km	5.43 g/cm^3	3.33×10^{23} kg	0.7×10^4	6×10^4	780 km
Venus	6051.8 km	5.24 g/cm^3	4.87×10^{24} kg	0.97×10^5	3.9 ×10^5	1250 km
Earth	6378.1 km	5.52 g/cm^3	5.97×10^{24} kg	1.2×10^5	4.8 ×10^5	1320 km
Mars	3389.5 km	3.93 g/cm^3	6.42×10^{23} kg	1.3×10^4	5.2×10^4	755 km
Jupiter	69911 km	1.33 g/cm^3	1.9×10^{27} kg	0.4×10^8	1.6×10^8	5623 km
Saturn	58232 km	0.69 g/cm^3	5.68×10^{26} kg	1.1×10^7	4.4×10^7	4072 km
Uranus	25362 km	1.27 g/cm^3	8.68×10^{25} kg	1.7×10^6	6.8×10^6	2553 km
Neptun	24622 km	1.64 g/cm^3	1.02×10^{26} kg	0.2×10^7	0.8×10^7	2659 km
Pluto	1188.3 km	1.86 g/cm^3	1.3×10^{22} kg	0.3×10^3	1.2×10^3	359 km

We apply Ex. (88)

$r_{cP} \approx ½\, A^{1/3} r_4 \approx ½\, A^{1/3}{\times}10^7$ cm = $½\, A^{1/3}{\times}100$ km,

where A is the number of P_k-"quarks$_3$" to estimate the radius of the naked P_k-"planet$_3$" Earth using approximate data from Table 2

$r_E \approx ½\, A^{1/3} r_4 \approx ½\, (4.8\ 10^5)^{1/3}{\times}100$ km $\approx$ 1320 km, (95)

while modern reference books indicate the radius of the inner core of planet Earth as ~ 1300 km.

Similarly, we estimate the radius of the naked "$star_3$" the Sun

$$r_S \approx ½\, A^{1/3} r_4 \approx ½\, (1.6\times10^{11})^{1/3}\times100 \text{ km} \approx 316\,000 \text{ km}. \quad (96)$$

According to modern reference data, the solar core extends from the center of the Sun to a distance of ~ 173 000 km.

These calculations show that the above-proposed method allows us to obtain estimates of the radii of the cores of astronomical objects that are close in order of magnitude to the known ones (i.e. obtained by other methods).

The last column of Table 2 shows the approximate radii of naked P_k-"$planets_3$" calculated using formula (88).

7. Comparison of the naked "Solar System" with a biological cell

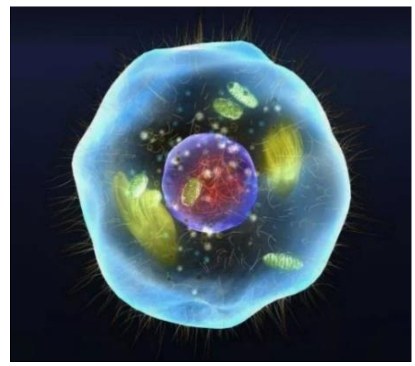

The naked "Solar System" considered in this article is in many ways similar to a biological cell (see Figure 6 and 7) not only in structure but also in internal content. For example, as shown in Table 2, the naked "$star_3$" the Sun consists of approximately one hundred sixty billion naked planetary P_k-"$quarks_3$" (1.6×10^{11}), approximately the same number of quarks are found in the nucleus of a biological cell.

As is known, genetic information in the form of DNA molecules is formed from the quarks located inside the nucleus of a biological cell. Therefore, it can be assumed that the core of the naked "$star_3$" the Sun also contains genetic information of the Solar System, which is woven from sixteen colored naked planetary P_k-"$quarks_3$" (see Table 1). The information content of the Algebra of stignatures and the Algebra of signatures was discussed in [1,2].

Similarly, the average naked P_k-"$planets_3$": Mercury, Venus, Earth, Mars, etc., consisting of about a million colored naked P_k-"$quarks_3$", are associated with organelles of the biological cell such as chloroplasts, peroxysomes and lysosomes, and the naked P_k-"giant $planets_3$": Jupiter (1.6×10^8), Saturn (4.4×10^7), Uranus (6.8×10^6) and Neptune (8×10^6) correspond to mitochondria.

Similar analogies between "galaxies" (megascopic level), "star" systems (macroscopic level), biological cells (microscopic level) and molecules (nanoscopic level) can be continued, for example, "galaxies" and "star" systems rotate, just as the cytoplasm in a living biological cell rotates, etc. But for a deeper understanding of the relationship between the various levels of Intelligibly Curved Being, it is necessary to devote a separate study.

8. Rotation of a naked P_k-"$planet_3$"

At this stage of the study, it is impossible to correctly construct a metric-dynamic model of the rotation of a naked P_k-"planet", since this phenomenon is associated with planetary gravity, which is planned to be considered in the next article. However, already at this stage, it is possible to formulate some prerequisites for creating such a model for an electrically neutral rotating naked P_k-"planet", based on [8].

As an example, let's consider the rotation of the neutral naked P_k-"$planet_3$" Earth. The material planet Earth makes a complete revolution around the Sun in approximately 365.26 solar days (i.e. revolutions around its axis, see Figure 10a) with an average speed of V_E ~ 110,000 km/h ≈ 30.5 km/s. A point on the Earth's equator travels 40,000 km in 24 hours (more precisely, in 23 hours 56 minutes 4.09 seconds), so it moves in a circle at an approximate speed of 40,000 km / 24 hours ≈ 1,666.7 km/h ≈ 465 m/s. The angular velocity of the Earth's rotation around its axis is ~ 7.3×10^{-5} radians per second (see Figure 10*b*).

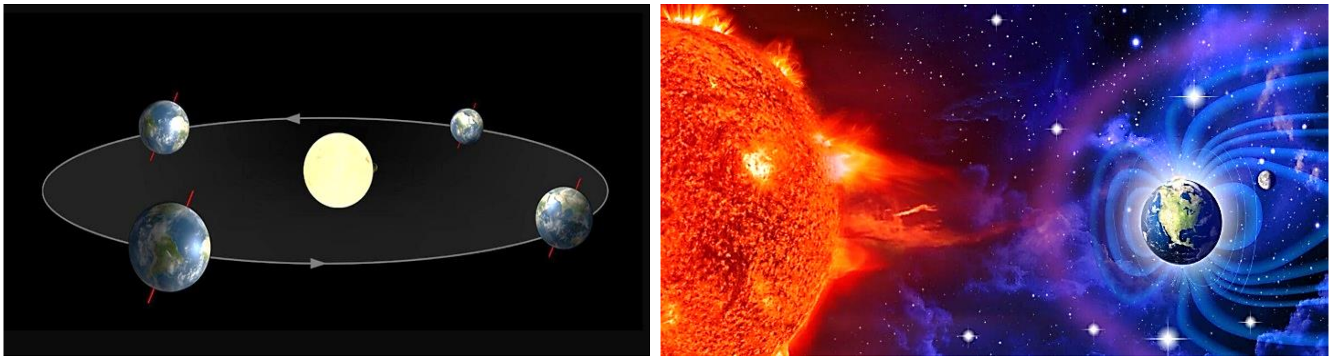

a) b)

Fig. 10. The material planet Earth moves around the material star Sun with a speed of ~30.5 km/s. The Earth also rotates around its axis with an angular velocity of 7.3×10^{-5} radians per second

On the other hand, this article puts forward a hypothesis that the electrically neutral naked P_k-"planet" Earth is the result of an additive superposition of approximately 480,000 planetary P_k-"quarks$_3$" of type (66) (see Table 2).

Based on the mathematical apparatus of the Algebra of signature [1,2,3,4,5,6,7,8,9], it can be assumed that ~ 480,000 planetary P_k-"quarks$_3$" are thus additively (i.e., on average) superimposed on each other, so that on average the metric-dynamic model of the outer shell of the electrically neutral valence rotating naked P_k-"planet$_3$" Earth is determined by the following set of generalized Kerr metrics (in Boyer–Lindquist coordinates) (see [8]):

Averaged outer shell of a rotating neutral naked valence P_k-"planet$_3$" Earth (97)

moving around the Sun at a speed of V_E
with a common signature

$$(+---)+(-+++)=(0\,0\,0\,0)$$

I $$ds_1^{(+a1)2}=\left(1-\frac{r_E r}{\rho}\right)c^2dt^2-\frac{\rho dr^2}{\Delta^{(a)}}-\rho d\theta^2-\left(r^2+a^2+\frac{r_E r a^2}{\rho}\sin^2\theta\right)\sin^2\theta\, d\phi^2+\frac{2r_E ra}{\rho}\sin^2\theta\, d\phi cdt, \quad (98)$$

H $$ds_2^{(+a2)2}=\left(1-\frac{r_E r}{\rho}\right)c^2dt^2-\frac{\rho dr^2}{\Delta^{(a)}}-\rho d\theta^2-\left(r^2+a^2+\frac{r_E r a^2}{\rho}\sin^2\theta\right)\sin^2\theta\, d\phi^2-\frac{2r_E ra}{\rho}\sin^2\theta\, d\phi cdt, \quad (99)$$

V $$ds_3^{(+b1)2}=\left(1+\frac{r_E r}{\rho}\right)c^2dt^2-\frac{\rho dr^2}{\Delta^{(b)}}-\rho d\theta^2-\left(r^2+a^2-\frac{r_E r a^2}{\rho}\sin^2\theta\right)\sin^2\theta\, d\phi^2+\frac{2r_E ra}{\rho}\sin^2\theta\, d\phi cdt, \quad (101)$$

H′ $$ds_4^{(+b1)2}=\left(1+\frac{r_E r}{\rho}\right)c^2dt^2-\frac{\rho dr^2}{\Delta^{(b)}}-\rho d\theta^2-\left(r^2+a^2-\frac{r_E r a^2}{\rho}\sin^2\theta\right)\sin^2\theta\, d\phi^2-\frac{2r_E ra}{\rho}\sin^2\theta\, d\phi cdt; \quad (102)$$

H′ $$ds_1^{(-a1)2}=-\left(1-\frac{r_E r}{\rho}\right)c^2dt^2+\frac{\rho dr^2}{\Delta^{(a)}}+\rho d\theta^2+\left(r^2+a^2+\frac{r_E r a^2}{\rho}\sin^2\theta\right)\sin^2\theta\, d\phi^2-\frac{2r_E ra}{\rho}\sin^2\theta\, d\phi cdt, \quad (103)$$

V $$ds_2^{(-a2)2}=-\left(1-\frac{r_E r}{\rho}\right)c^2dt^2+\frac{\rho dr^2}{\Delta^{(a)}}+\rho d\theta^2+\left(r^2+a^2+\frac{r_E r a^2}{\rho}\sin^2\theta\right)\sin^2\theta\, d\phi^2+\frac{2r_E ra}{\rho}\sin^2\theta\, d\phi cdt, \quad (104)$$

H $$ds_3^{(-b1)2}=-\left(1+\frac{r_E r}{\rho}\right)c^2dt^2+\frac{\rho dr^2}{\Delta^{(b)}}+\rho d\theta^2+\left(r^2+a^2-\frac{r_E r a^2}{\rho}\sin^2\theta\right)\sin^2\theta\, d\phi^2-\frac{2r_E ra}{\rho}\sin^2\theta\, d\phi cdt, \quad (105)$$

I $$ds_4^{(-b2)2}=-\left(1+\frac{r_{E6} r}{\rho}\right)c^2dt^2+\frac{\rho dr^2}{\Delta^{(b)}}+\rho d\theta^2+\left(r^2+a^2-\frac{r_E r a^2}{\rho}\sin^2\theta\right)\sin^2\theta\, d\phi^2+\frac{2r_E ra}{\rho}\sin^2\theta\, d\phi cdt; \quad (106)$$

The substrate

of the rotating naked valence P_k-"planet$_3$"
with common signature

$$(+---)+(-+++)=(0\,0\,0\,0)$$

i $$ds_5^{(+)2}=c^2dt^2-\frac{\rho dr^2}{r^2+a^2}-\rho d\theta^2-(r^2+a^2)\sin^2\theta\, d\phi^2, \quad (107)$$

j $$ds_5^{(-)2}=-c^2dt^2+\frac{\rho dr^2}{r^2+a^2}+\rho d\theta^2+(r^2+a^2)\sin^2\theta\, d\phi^2. \quad (108)$$

where $\rho = r^2 + a^2 cos^2\theta$, $\Delta^{(a)} = r^2 - r_E r + a^2$, $\Delta^{(b)} = r^2 + r_E r + a^2$; (109)

$a = \frac{r_E V_E}{2c}$ is ellipticity parameter;

$V_E \approx 30{,}5$ km/s is speed of movement of the naked P_k-"planet$_3$" Earth;

$r_E \approx 1320$ km is radius of the core of the naked P_k-"planet$_3$" Earth (see the last column in Table 2).

We recall (see § 5.2 in [3]) that averaged metrics with opposite signatures (+ – – –) and (– + + +) describe metric-dynamic states of the $\lambda_{6,7}$-vacuum layers that are rotated (or phase-shifted) by 90° relatives to each other.

A separate, extensive study should be devoted to the metric-dynamic models of rotating electrically neutral naked P_k -"planets$_3$" and P_k-"stars$_3$". Here we will only note that, for example, the metric-dynamic model of the outer shell of the electrically neutral valence naked P_k-"planet$_3$" Earth (98) – (109) should lead to a description of the magnetic field of this planet (see Figs. 10b and 11).

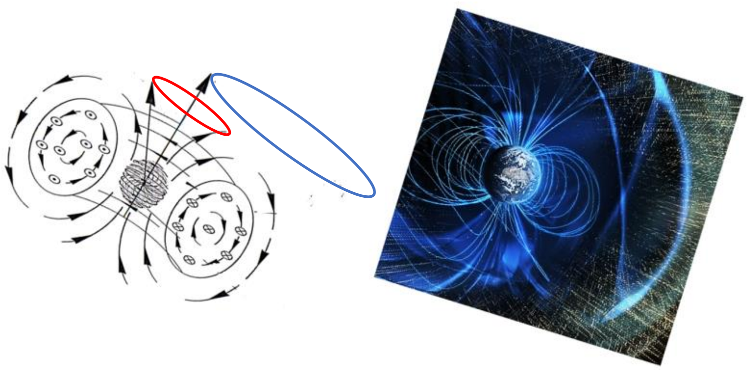

Fig. 10. Schematic representation of subcont-antisubcont currents determining the lines of force of the geometrized magnetic field of a moving neutral valence naked P_k-"planet"

CONCLUSION

"Physics is Geometry"
John Archibald Wheeler [11]

This tenth part of "Geometrized Vacuum Physics (GVPh) based on the Algebra of signature (AS)" [1,2,3,4,5,6,7,8,9] partly considers metric-dynamic models of electrically neutral valence naked P_k-"planets" and P_k-"stars", which follow from the hierarchical cosmological model proposed in [6].

The concept of naked stable spherical $\lambda_{6,7}$-vacuum formations (P_k-"planets" and P_k-"stars") implies the conditional absence of pico-, nano- and microscopic $\lambda_{m,n}$-vacuum formations (i.e. elementary "particles", "molecules", "cells", etc.) in the studied region of $\lambda_{6,7}$-vacuum. That is, only curvatures of macroscopic areas of $\lambda_{6,7}$-vacuum of planetary and stellar scale are considered, provided that small fluctuations of $\lambda_{m,n}$-vacuum are not taken into account. It is assumed that the next article will consider the mechanism of attraction of small "particles" by naked P_k-"planets" and P_k-"stars", i.e. another attempt will be made to unravel the mystery of planetary and stellar gravity based on the mathematical apparatus of the GVPh and AS, presented in [1,2,3,4,5,6,7,8,9].

It is shown that 16 colored naked planetary P_k-"quarks$_3$" with the corresponding signatures (65) are sufficient for constructing metric-dynamic models of all stable $\lambda_{6,7}$-vacuum formations of stellar-planetary scale. Colored planetary P_k-"quarks$_3$" are presented in Table 1, from them naked planetary P_k-"baryons$_3$", P_k-"mesons$_3$", P_k-"atoms$_3$" and P_k-"molecules$_3$" can be composed by analogy with the construction of picoscopic elements of the Standard Model of elementary "particles" in the articles [6,7,8,9].

A comparison of naked P_k-"planets$_3$" and P_k-"stars$_3$" with material astronomical objects of the Solar System is given. A method for estimating the number of planetary P_k-"quarks$_3$" inside the material Sun and material planets of the Solar System is proposed. Calculations using this method led to results similar in order of magnitude to known modern reference data on the parameters of material planets and the Sun.

A number of similar features between the naked "Solar System" and a biological cell are identified. It is noted that the naked P_k-"star$_3$" Sun can be compared to the nucleus of a biological cell, and the naked P_k-"planets$_3$" of this system are similar to other organelles of a biological cell, such as, for example, mitochondria and lysosomes.

A preliminary metric-dynamic model of a rotating electrically neutral valence naked P_k-"planet$_3$" is proposed.

As has been repeatedly noted within the framework of the GVPh and AS [1,2,3,4,5,6,7,8,9], a completely geometrized description of the “star-planetary” level of organization of the curved $\lambda_{6,7}$-vacuum has its own characteristics, but is in many ways similar to the geometrized description of all other layers of the bottomless emptiness (vacuum). By comprehending one of the levels (or layers) of curvatures of the $\lambda_{m,n}$-vacuum, we simultaneously supplement the ideas about all other stable and unstable $\lambda_{m,n}$-vacuum formations of various scales, since they are fractally repeated in each other.

We hope that this article is another step towards the implementation of the program of full geometrization physics of Clifford-Einstein-Wheeler.

ACKNOWLEDGEMENTS

I would like to express my sincere gratitude to Gavriel Davidov, David Reid, Tatyana Levy, Eliezer Rahman, David Kogan, Gennady Ivanovich Shipov, Evgeny Alekseevich Gunakedv, Carlos J. Rojas, Alexander Maslov, Alexander Bolotov, Alexander Bindiman and Ilya Kolomin for their assistance.

REFERENCES

[1] Batanov-Gaukhman, M. (2023). Geometrized Vacuum Physics. Part I. Algebra of Stignatures. Avances en Ciencias e Ingeniería, 14 (1), 1-26, https://www.executivebs.org/publishing.cl/avances-en-ciencias-e-ingenieria-vol-14-nro-1-ano-2023-articulo-1/; and Preprints, 2023060765. https://doi.org/10.20944/preprints202306.0765.v3, and viXra:2403.0035.
[2] Batanov-Gaukhman, M. (2023).Geometrized Vacuum Physics. Part II. Algebra of Signatures. Avances en Ciencias e Ingeniería, 14 (1), 27-55, https://www.executivebs.org/publishing.cl/avances-en-ciencias-e-ingenieria-vol-14-nro-1-ano-2023-articulo-2/: and Preprints, 2023070716, https://doi.org/10.20944/preprints202307.0716.v1, and viXra:2403.0034.
[3] Batanov-Gaukhman, M. (2023). Geometrized Vacuum Physics. Part III. Curved Vacuum Area. Avances en Ciencias e Ingeniería Vol. 14 nro 2 año 2023 Articulo 5, https://www.executivebs.org/publishing.cl/avances-en-ciencias-e-ingenieria-vol-14-nro-2-ano-2023-articulo-5/; and Preprints 2023, 2023080570. https://doi.org/10.20944/prerints202308.0570.v4, and viXra:2403.0033.
[4] Batanov-Gaukhman, M. (2024). Geometrized Vacuum Physics. Part IV: Dynamics of Vacuum Layers. Avances en Ciencias e Ingeniería Vol. 14 nro 3 año 2023 Articulo 1 https://www.executivebs.org/publishing.cl/avances-en-ciencias-e-ingenieria-vol-14-nro-3-ano-2023-articulo-1/, and Preprints.org. https://doi.org/10.20944/preprints202310.1244.v3, and viXra:2403.0032.
[5] Batanov-Gaukhman, M. (2024). Avances en Ciencias e Ingeniería Vol. 14 nro 3 año 2023 Articulo 2 https://www.executivebs.org/publishing.cl/avances-en-ciencias-e-ingenieria-vol-14-nro-3-ano-2023-articulo-2/, and viXra:2405.0002.
[6] Batanov-Gaukhman, M. (2024) Geometrized Vacuum Physics Part 6: Hierarchical Cosmological Model, Avances en Ciencias e Ingeniería Vol. 14 nro 4 año 2023 https://www.executivebs.org/publishing.cl/avances-en-ciencias-e-ingenieria-vol-14-nro-4-ano-2023-articulo-3/ and viXra:2408.0010.
[7] Batanov-Gaukhman, M. (2024). Geometrized Vacuum Physics Part 7: "Electron" and "Positron", viXra:2409.0097.
[8] Batanov-Gaukhman, M. (2024). Geometrized Vacuum Physics Part 8: Inertial Electromagnetism of Moving "Particles", viXra:2409.0097.

[9] Batanov-Gaukhman, M. (2025). Geometrized Vacuum Physics Part 9: Neutrino, viXra:2501.0059.[10] Shipov, G. (1998). ”A Theory of Physical Vacuum”. Moscow ST-Center, Russia ISBN 5 7273-0011-8.
[10] Shipov, G. (1998). ”A Theory of Physical Vacuum”. Moscow ST-Center, Russia ISBN 5 7273-0011-8.
[11] Misner, C. and Wheeler, J. (1957). Classical Physics as Geometry: Gravity, Electromagnetism, Unquantized Charge, and Mass as Properties of Curved Empty Space. Annals Phys. 2 (1957) 525–603, DOI:10.1016/0003-4916(57)90049-0.
[12] Wheeler, J. “Gravity, Neutrinos, and the Universe.” Moscow: Foreign Literature Publishing House, 1962.

Appendix 1

A partial list of the small satellites of the planets in the Solar System

Taken from the website "The Solar System Wiki"

№	Astronomical object	Diameter km	№	Astronomical object	Diameter km	№	Astronomical object	Diameter km
1	Ganymede	1,527[5]	41	Despina	148[5]	81	S / 2002 N 5	33.45[29][27]
2	Titan	1,522.8[6]	42	Himalia	139.6[20]	82	Stefano	32[26][27]
3	Callisto	1,468.8[7]	43	Xiangliu	136[21][22]	83	Atlas	30.2[31]
4	Io	1,212[8]	44	Portia	135[19]	84	Ananke	29.1[20]
5	Moon	1,169.4[6]	45	Hãunu	122[13]	85	Paaliaq	29[17]
6	Europa	1,157.8[6]	46	Epimetheus	116.4[5]	86	Telesto	28.8[32]
7	Triton	1,122.8[7]	47	G!ò'é !Hú	112[23]	87	Pan	28[33]
8	Titania	1,062.2[7]	48	Thebe	98.6[5]	88	Perdita	26.6[34]
9	Rhea	700[9]	49	Juliet	94[19]	89	Mab	24.8[34]
10	Oberon	504.2[7]	50	Belinda	90[19]	90	Phobos	22.16[35]
11	Iapetus	471.6[6]	51	Prometheus	86.2[5]	91	Francisco	22[26][27]
12	Charon	443[9]	52	Caliban	84[24]	92	S/2021 N 1	21.95[29][27]
13	Umbriel	418[10]	53	Pandora	81.2[5]	93	Leda	21.5[20]
14	Ariel	396.4[7]	54	Cressida	80[19]	94	Ferdinand	21[26][27]
15	Dione	~356[11]	55	Thalassa	80[5]	95	Margaret	20[26][27]
16	Tethys	340[5]	56	Elara	79.9[20]	96	Calypso	19.2[32]
17	Dysnomia	~320[12]	57	Rosalind	72[19]	97	Ymir	18.8[29][36]
18	Enceladus	284[13]	58	Desdemona	64[19]	98	Trinculo	18[26][27]
19	Miranda	270[7]	59	Halimeda	~62[25]	99	Kiviuq	18[37]
20	Vant	213[7]	60	Naiad	58[5]	100	Cupid	17.8[34]
21	Proteus	213[14]	61	Pasiphae	57.8[20]	101	Themisto	16.4[17]
22	Mimas	210[14]	62	Prospero	52.8[26][27]	102	Adrastea	16.4[5]
23	Ilmara	~200[15]	63	Bianca	51[19]	103	Tarvos	15.5[37]
24	Nereid	192[5]	64	Neso	48.8[25][28]	104	Ijirak	13.5[37]
25	Hiaka	186[16]	65	Setebos	47[26][27]	105	Deimos	12.54[35]
26	Actaea	183.4[17]	66	Carme	46.7[20]	106	Kerberos	12[5]
27	Hyperion	178.4[5]	67	Sao	~44[25]	107	S/2023 U 1	10.6[29][27]
28	Phoebe	1,527[5]	68	Siarnaq	43.2[17]	108	Erriapus	10.5[37]
29	S/2012 (38628) 1	1,522.8[6]	69	Metis	43[5]	109	Styx	10.4[5]
30	S/2005 (55637) 1	1,468.8[7]	70	Ophelia	43[19]	110	S / 2002 N 5	33.45[29][27]
31	Weywot	1,212[8]	71	Lysithea	42.2[20]	111	Stefano	32[26][27]
32	Larissa	1,169.4[6]	72	Laomedeia	~42[25]	112	Atlas	30.2[31]
33	S/2018 (532037)	1,157.8[6]	73	Cordelia	40[19]	113	Ananke	29.1[20]
34	Sycorax	1,122.8[7]	74	Psamathe	~40[25]	114	Paaliaq	29[17]
35	Janus	1,062.2[7]	75	Albiorix	37[17]	115	Telesto	28.8[32]
36	S/2015 (136472)	~175[18]	76	Hydra	37[5]	116	Pan	28[33]
37	Amalthea	167[5]	77	Helen	36[7]	117	Perdita	26.6[34]
38	Puck	162[19]	78	Nyx	36[5]	118	Mab	24.8[34]
39	Namaka	~160[12]	79	Sinope	35[20]	119	Phobos	22.16[35]
40	Galatea	158[5]	80	Hippocamp	34.8[30]	120	Francisco	22[26][27]

№	Astronomical object	Diameter km	№	Astronomical object	Diameter km	№	Astronomical object	Diameter km
121	S/2021 N 1	21.95[29]	159	Styx	10.4[5]	198	Narvi	5.4[38][37]
122	Leda	21.5[20]	160	Callirrhoe	10.2[17]	199	Aegir	5[37]
123	Ferdinand	21[26][27]	161	Hyrrokkin	7.8[38][37]	200	Eggther	5[37]
124	Margaret	20[26][27]	162	Daphnis	7.6[32]	201	Greep	5[37]
125	Calypso	19.2[32]	163	Thrymr	7.4[38][37]	202	Hati	5[37]
126	Ymir	18.8[29]	164	Mundilfari	7.5[38][37]	203	Loge	5[37]
127	Trinculo	18[26][27]	165	Praktika	7[20]	204	Skoll	5[37]
128	Kiviuq	18[37]	166	Kalike	6.9[20]	205	S/2019S1	5[37]
129	Cupid	17.8[34]	167	Megaclite	6.6[39][40][38]	206	Aoede	4.6[38][40]
130	Themisto	16.4[17]	168	Skathi	6.6[37]	207	Helike	4.6[38][40]
131	Adrastea	16.4[5]	169	Bergelmir	6.5[38][37]	208	Thyon	4.6[38][40]
132	Tarvos	15.5[37]	170	Narvi	6[37]	209	Alvaldi	4.5[37]
133	Ijirak	13.5[37]	171	Aegir	6[37]	210	S/2006S1	4.5[37]
134	Deimos	12.54[35]	172	Styx	6[38][40]	211	Pallene	4.46[32]
135	Kerberos	12[5]	173	Callirrhoe	5.8[38][37]	212	Harpalike	4.4[41][40]
136	S/2023 U 1	10.6[29]	174	Hyrrokkin	5.8[38][37]	213	Euanthe	4[38][40]
137	Erriapus	10.5[37]	175	Daphnis	5.8[38][37]	214	Farbauti	4[37]
138	rgaret	10.4[5]	176	Thrymr	5.5[37]	215	Narvi	5.4[38][37]
139	Calypso	10.2[17]	177	Mundilfari	5.4[38][37]	216	Aegir	5[37]
140	Ymir	7.8[38][37]	178	Praktika	5[37]	217	Eggther	5[37]
141	Trinculo	7.6[32]	179	Kalike	10.4[5]	218	Greep	5[37]
142	Kiviuq	21.9[29]]	180	Megaclite	10.2[17]	219	Hati	5[37]
143	Cupid	21.5[20]	182	Skathi	7.8[38][37]	220	Loge	5[37]
144	Themisto	21[26][27]	183	Tarqeq	7.6[32]	221	Skoll	5[37]
145	Adrastea	20[26][27]	184	Bebhionn	7.4[38][37]	222	S/2019S1	5[37]
146	Tarvos	19.2[32]	185	Fornjot	7.5[38][37]	223	Aoede	4.6[38][40]
147	Ijirak	18.8[29]	186	Germippe	7[20]	224	Helike	4.6[38][40]
148	Deimos	18[26][27]	187	Bestla	6.9[20]	225	Thyon	4.6[38][40]
149	Kerberos	18[37]	188	Suttungr	6.6[39][40][38]	226	Alvaldi	4.5[37]
150	S/2023 U1	17.8[34]	189	Kari	6.6[37]	227	S/2006S1	4.5[37]
151	Erriapus	16.4[17]	190	Bergelmir	6.5[38][37]	228	Pallene	4.46[32]
152	S/2021 N 1	16.4[5]	191	Styx	6[37]	229	Harpalike	4.4[41][40]
153	Leda	15.5[37]	192	Callirrhoe	6[37]	230	Euanthe	4[38][40]
154	Ferdinand	13.5[37]	193	Hyrrokkin	6[38][40]	231	Farbauti	4[37]
155	Margaret	12.54[35]	194	Daphnis	5.8[38][37]	232	Narvi	5.4[38][37]
156	Calypso	12[5]	195	Thrymr	5.8[38][37]	233	Aegir	5[37]
157	Ymir	10.6[29]	196	Mundilfari	5.8[38][37]	234	Eggther	5[37]
158	Trinculo	10.5[37]	197	Praktika	5.5[37]	235	Greep	5[37]